THERMOECONOMIC ANALYSIS OF A BRAYTON AND RECOMPRESSION OF A SUPERCRITICAL CO_2 COMBINED POWER CYCLE IN HILLA

2024
MASTER THESIS
MECHANICAL ENGINEERING

Zainalabden Oday Hatm MOHMEDALI ALNAJFY

Thesis Advisors
Assist. Prof. Dr. Erhan KAYABAŞI
Assist. Prof. Dr. Ali IBRAHIM

THERMOECONOMIC ANALYSIS OF A BRAYTON AND RECOMPRESSION OF A SUPERCRITICAL CO_2 COMBINED POWER CYCLE IN HILLA

Zainalabden Oday Hatm MOHMEDALI ALNAJFY

Thesis Advisors

Assist. Prof. Dr. Erhan KAYABAŞI

Assist. Prof. Dr. Ali IBRAHIM

T.C

Karabuk University

Institute of Graduate Programs

Department of Mechanical Engineering

Prepared as

Master Thesis

KARABUK

January 2024

I certify that in my opinion the presented thesis that has been submitted by Zainalabden Oday Hatm MOHMEDALI ALNAJFY titled “THERMOECONOMIC ANALYSIS OF A BRAYTON AND RECOMPRESSION OF A SUPERCRITICAL CO_2 COMBINED POWER CYCLE IN HILLA” is fully adequate in scope and in quality as a thesis for the degree of Master of Science.

Assist. Prof. Dr. Erhan KAYABAŞI .....
Thesis Advisor, Department of Mechanical Engineering

Assist. Prof. Dr. Ali IBRAHIM .....
2. Thesis Advisor, Department of Mechanical Engineering

This thesis is accepted by examining committee with the unanimous vote in the Dept. of Mechanical Engineering as Master of Science thesis. January 8, 2024.

Examining Committee Members (Institutions)	Signature
Chairman : Prof. Dr. Engin GEDIK (KBU)	.....
Member : Assist. Prof. Dr. Abdulrazzak AKROOT (KBU)	.....
Member : Assist. Prof. Dr. Erhan KAYABAŞI (KBU)	.....
Member : Assist. Prof. Dr. Fatih UYSAL (SUBU)	.....

The degree of Master of Science by the thesis that has been submitted was approved by the Administrative Board of Institute of Graduate Programs, Karabuk University.

Assoc. Prof. Dr. Zeynep ÖZCAN .....
Director of the Institute of Graduate Programs

"I declare that all the information that has been presented in this thesis was gathered and presented in accordance with ethical principles and academic regulations and I have according to requirements of those regulations and principles that were cited all those which don't originate in this work too."

Zainalabden Oday Hatm MOHMEDALI ALNAJFY

ABSTRACT

M. Sc. Thesis

THERMOECONOMIC ANALYSIS OF A BRAYTON AND RECOMPRESSION OF A SUPERCRITICAL CO_2 COMBINED POWER CYCLE IN HILLA

Zainalabden Oday Hatm MOHMEDALI ALNAJFY

Karabuk University
Institute of Graduate Programs
The Department of Mechanical Engineering

Thesis Advisors:
Assist. Prof. Dr. Erhan KAYABAŞI
Assist. Prof. Dr. Ali IBRAHIM
January 2024, 57 pages

In this study, the thermoeconomic analysis of a combined power cycle consisting of Bryton power cycle and sCO2 cycle was examined. Brayton cycle was used as the topping cycle and sCO2 cycle was used as the bottoming cycle. At the Hilla gas station, the waste heat resulting from power generation is transferred to the supercritical CO2 cycle, which operates as a closed loop, through a Bryton cycle that uses methane as fuel. The 1st and 2nd law analyzes of thermodynamics were applied to this study and the energy exergy, economy and environment analyzes of the combined cycle were carried out. As a result of the study, the total energy production of the system, the cost of the electricity produced, the investment costs of the system and its environmental effects in 6 different operating regimes during the year were obtained. According to the results obtained, it was observed that the highest total electricity production was

42.9 MW, 26.83 MW from the Brayton cycle and 16.11 MW from the sCO2 cycle. The lowest electricity production values were observed to be 19.9 MW in total, 11.5 MW from the Brayton cycle and 8.4 MW from the sCO2 cycle. Total combined energy efficiency was between 40% and 43.3%. Exergy efficiency was between 47.6% and 55.53%. The electricity production cost was found to be 0.0145 $/kWh and 0.0162 $/kWh, which is well below the market values. Finally, when the environmental impacts were examined, it was observed that CO2 emissions were reduced by 2 to 4.81 tons/day.

Key Words : Supercritical CO_2 (sCO_2) power cycle, Waste heat recovery system performance, Energy extraction

Science Code : 91408

ÖZET

Yüksek Lisans Tezi

HİLLA'DA BRAYTON VE SIKIŞTIRMALI sCO_2 BİRLEŞİK GÜÇ ÇEVRİMİNİN TERMOEKONOMİK ANALİZİ

Zainalabden Oday Hatm MOHMEDALI ALNAJFY

Karabük Üniversitesi
Lisansüstü Eğitim Enstitüsü
Makine Mühendisliği Anabilim Dalı

Tez Danışmanları:
Dr. Öğr. Üyesi Erhan KAYABAŞI
Dr. Öğr. Üyesi Ali IBRAHIM
Ocak- 2024, 57 sayfa

Bu çalışmada Bryton güç çevrimi ve sCO_2 çevriminden oluşan bir bişleşik güç çevriminin termoekonomik analizi incelenmiştir. Üst çevrim olarak Brayton çevrimi ve alt çevrim olarak sCO_2 çevrimi kullanılmıştır. Hilla gaz istanyonunda yakıt olarak metan kullanan bir Bryton çevirimi ile güç üretiminden ortaya çıkan atık ısı kapalı çevrim olarak çalışan süperkritik CO_2 çevrimine aktarılmaktadır. Termodinamiğin 1. ve 2. yasa analizleri bu çalışmaya uygulanmış ve birleşik çevrimin enerji ekserji ve ekonomi ve çevre analizleri gerçekleştirilmiştir. Çalışma sonucunda yıl içerisinde meydana gelen 6 farklı çalışma rejimlerinde sistemin toplam enerji üretimi, üretilen elektriğin maliyeti, sistemin yatırım maliyetleri ve çevresel etkileri eldedilmiştir. Elde edilen sonuçlara göre en yüksek toplam elektrik üretiminin 26.83 MW'ı Brayton çevriminden, 16.11 MW'ı sCO_2 çevriminden olmak üzere toplam 42.9 MW olduğu gözlemlenmiştir. En düşük elektrik üretim değerleri ise 11.5 MW'ı Brayton

çevriminden 8.4 MW'ı sCO_2 çevriminden olmak üzere toplam 19.9 MW olduğu gözlemlenmiştir. Toplam birleşik energy verimliliği ise 40% ile 43.3% aralığında gerçekleşmiştir. Ekserji verimi ise 47.6% ile 55.53% aralığında meydana gelmiştir. Elektrik üretim maliyeti ise piyasa değerlerinin çok altında bir değer olan 0.0145 $/kwh ile 0.0162 $/kWh aralığında bulunmuştur. Son olarak çevresel etkiler incelendiğinde 2 ile 4.81 ton/gün CO_2 salınımı azaltıldığı gözlemlenmiştir.

Anahtar Kelimeler : Süperkritik CO_2 (sCO_2) güç çevrimi, Atık ısı geri kazanım sistemi performansı, Enerji geri kazanımı.

Bilim Kodu : 91408

ACKNOWLEDGMENT

First and foremost, I thank Almighty Allah, the Almighty Merciful, for giving me strength and knowledge for the completion of this work.

I would like to acknowledge and give my warmest thanks to my supervisors Assist. Prof. Dr. Erhan KAYABAŞI and Assist. Prof. Dr. Ali IBRAHIM who made this work possible. Their guidance and advice carried me through all the stages of writing my project.

Thanks, extend to the staff of Hilla Gas Station specially Eng. Jaber and Eng. Radhwan. Also, I would like to express my sincere gratitude to my friend Ibrahim.

To my father Consultant engineer Oday Hatem Hamza, the first teacher in my life. I learned great things from him, Thanks for being there for us.

To my beloved mother, my sweety, my inspiration, which always takes my hand and never leave it. Thank you for being my mother.

To my brothers (Mohammed, Ali, Hatem, Abdullah) and sisters (Fatima). the closest people to myself, those who filled my life with challenges and overcoming difficulties those who never hesitate to help me.

To my wife and daughter, the source of support, happiness and encouragement, my world is full of smiles whenever you are with me.

CONTENTS

Page

Page

LIST OF FIGURES

Page

LIST OF TABLES

Page

SYMBOLS AND ABBREVITIONS INDEX

SYMBOLS

$\dot{m}$: Mass flow rate (kg/sec)

T : Temperature (C)

p : Pressure (bar)

cp : Specific heat capacity (kJ/kg.K)

$\dot{Q}$: Heat transfer per unit time (Watt)

$\dot{W}$: Work done by the control volume per unit time (Watt)

h : Specific enthalpy (kJ/kg)

S : Specific entropy (kJ/kg.K)

T_0 : Boundary temperature (C)

CRF : Capital Recovery Factor

i : Interest rate (considered to be 6%)

n : System lifetime (considered to be 20 years)

k : Component

e^{PH} : Physical exergy (kJ/kg)

e^{CH} : Chemical exergy (kJ/kg)

e^{KN} : Kinetic energy exergy (kJ/kg)

e^{PT} : Potential exergy (kJ/kg)

$\dot{E}_{q,j,k}$: Heat transfer exergy (Watt)

$\dot{W}_k$: Power (Watt)

$\dot{E}_{i,k}$: Exergy inlet (Watt)

$\dot{E}_{e,k}$: Exergy exit (Watt)

C_C : Emission factor (tons/TJ)

H_V : Gross calorific value (TJ/kiloton)

C_C : Carbon emissions factor

ABBREVITIONS

HRU : Heat Rejection Unit

HTR : High Temperature Recuperator

HX : Heat Exchanger

LTR : Low Temperature Recuperator

PCHE :

REC : Recuperator

RRC : Recompressed Recuperative Cycle

sCO2 : Supercritical Carbon Dioxcide

SRC : Simple Recuperative Cycle

TIT : Turbine Inlet Temperature

TOT : Turbine Outlet Temperature

WHR : Waste Heat Recover

LCOE : levelized cost of electricity

GT : Gas Turbine

PART 1

INTRODUCTION

In the past sixty years, with the increase in population and economic activity, the global electricity demand has risen continuously, which has caused a serious environmental impact Increasingly extreme weather events and rising sea levels are unmistakable signs of one of the biggest challenges of our time: climate change. At the same time, around 850 million people still live without reliable access to electricity, which is the foundation of sustainable development. Thus, how to efficiently deal with these challenges is a durable hot topic.

Of these five principal greenhouse gases, carbon dioxide is by far the most significant in terms of both overall emissions and rate of growth. By the time the first Mauna Loa samples were examined in 1958, CO_2 levels had increased by 35 ppm from the 280 ppm pre-industrial level. Today's CO_2 concentration is 410 ppm, up an additional 95 ppm in the last 60 years[1].

On March 22, 2019 the concentration of atmospheric carbon dioxide (CO_2) reached its fourth-highest yearly growth by the end of 2018, according to data from NOAA's atmospheric observatory at Mauna Loa, which has been keeping records for 60 years.

According to a recent analysis of air samples gathered by NOAA's Global Monitoring Division (GMD), carbon dioxide increased by 2.87 parts per million (ppm) at the mountaintop observatory during 2018, rising from an average of 407.05 ppm on January 1, 2018, to 409.92 ppm on January 1, 2019.

Therefore, three of the last four years' biggest yearly gains have taken place, as shown in Figure (1) [2].

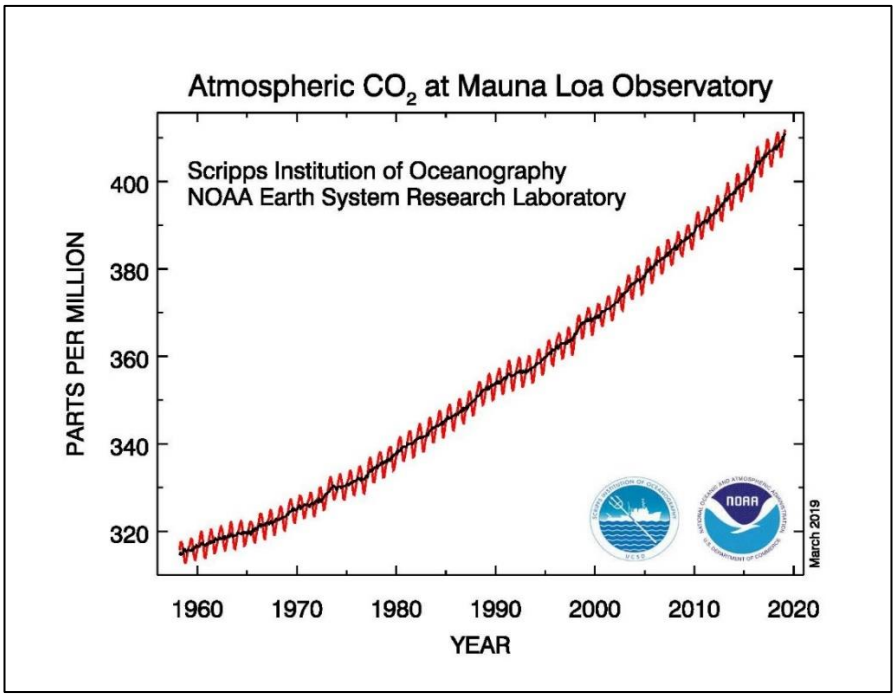

Figure 1.1. A chart showing the increase in the presence of carbon dioxide in the atmosphere (in parts per million) over the past 60 years.

In 2022, British Petroleum (BP) has created a scheme in which the sources of energy production from fossil fuels, nuclear energy, coal, wind and solar energy are compared, as shown in Figure (2)[3].

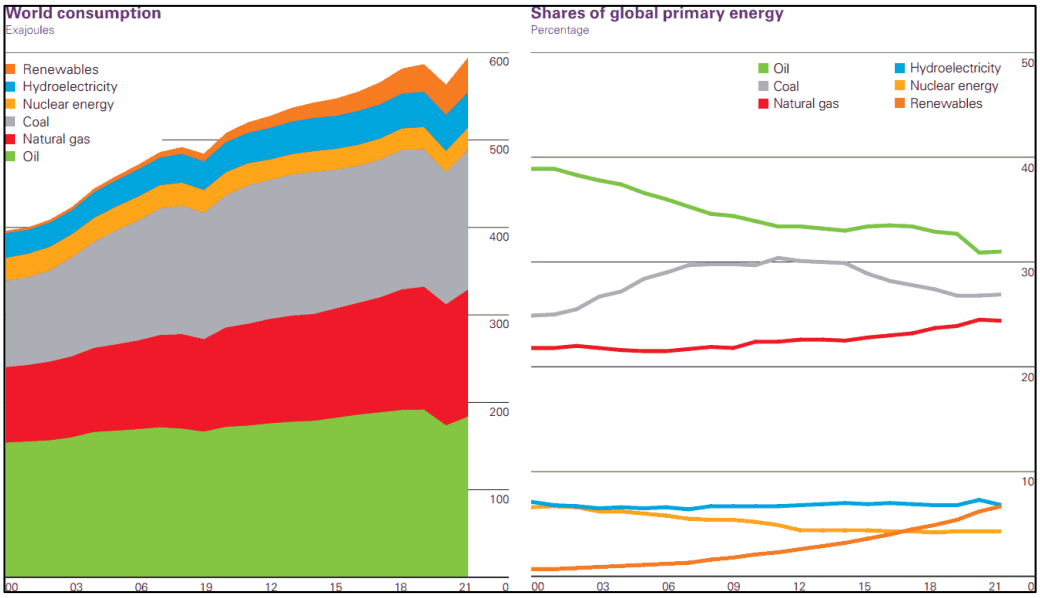

Figure 1.2. World primary energy consumption by source Renewables include solar, wind, geothermal, biomass, and other.

It turns out that the world is still mainly dependent on fossil fuels as well as coal, with clear growth in the use of renewable energy, and this is something expected due to the increasing energy demand, so we should consider developing those plants or taking advantage of the wasted energy in all fields to reduce their environmental damage and have an economic return in energy production [3].

In general, there are two ways to balance the environmental issue and the increase of electricity:

- Use recuperation heat or renewable energy sources to produce electricity. It is seen as an important first step toward future energy saving and emission reduction.
- Increase energy conversion efficiency. To create electricity more effectively while using fewer traditional energy fuels, alternative power cycles, including the supercritical water-steam Rankine cycle, organic Rankine cycle (ORC), and supercritical Brayton cycle, have been developed. It has been widely utilized to produce electricity using the supercritical water-steam cycle, which is powered by coal, natural gas, nuclear, and solar energy.

1.1. WASTE HEAT RECOVERY

The waste heat that is released into the environment has a high energy value and is also heavily polluted, which contributes to global warming. The process efficiency can be greatly improved and the primary energy consumption can be decreased by recovering this waste heat for specific uses [4].

Particularly significant are industrial operations, thermal engines, and mechanical devices that could benefit from such energy-saving potential [5].

In general, waste heat resources come in a wide variety of types and forms. According to the study by Galanis et al. [6], waste energy from industrial processes is released into the environment through four main states of matter: liquid streams between 50 °C and 300 °C, exhaust between 150 °C and 800 °C, steam between 100 °C and 250 °C,

as well as the process gases and vapors between 80 °C and 500 °C. Furthermore, the majority of the energy used for most end uses is waste heat that is low-temperature (350 °C). Evaluations demonstrate that 63% of waste heat streams form at temperatures below 100 °C, as depicted in Figure (3), Evaluations show that 63% of waste heat streams originate at temperatures below 100 °C, and the energy sector, which is followed by the commercial and transportation sectors in terms of production, produces the most of these waste heat streams [7].

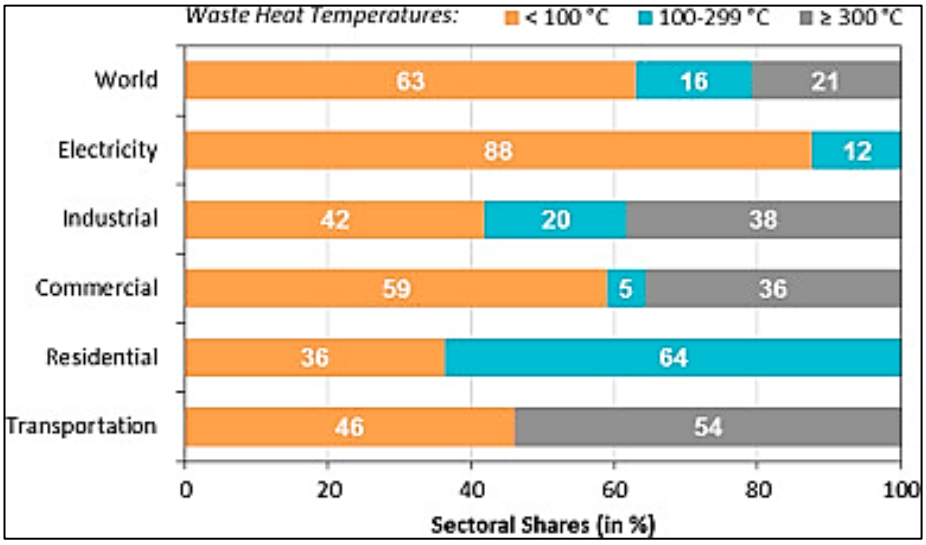

Figure 1.3. Sectoral shares of worldwide waste heat distribution.

The energy from waste heat can be recovered in a variety of ways from a thermodynamic perspective. Waste heat and other fluids, such as the heat transfer fluids used in the heating and cooling process, can directly exchange heat [8]. A thermodynamic cycle is used to transform waste heat into useful power. The high-temperature side of the waste heat can be employed as a heat source to warm the working fluid and create a gas phase with a specific temperature and pressure. It is possible to undertake expansion work using this working fluid or the waste heat fluid itself [9].

For specific applications, like distributed energy systems, another way is to use a heat pump to raise the temperature of the waste heat to the desired level. The low quality, fluctuation, and intermittency of heat sources, inefficiencies in the energy conversion

process, and cascading use of many energy sources are just a few of the difficulties that these diversified paths encounter.

1.2. BARRIERS TO WASTE HEAT RECOVERY

The use of waste heat as an energy source depends on many factors that make waste heat recovery very difficult, such as the principle of operation of heat recovery facilities, the characteristics of the waste heat source, and fluctuations and discontinuities compared to conventional heat sources, which severely affects the stability of the recovery system operation, Each method of waste heat recovery is posed with different problems, thus, the technologies face several barriers.

Waste heat is known to mainly originate from two types of sources, i.e., fossil fuel and renewable energy as shown in Figure (4).

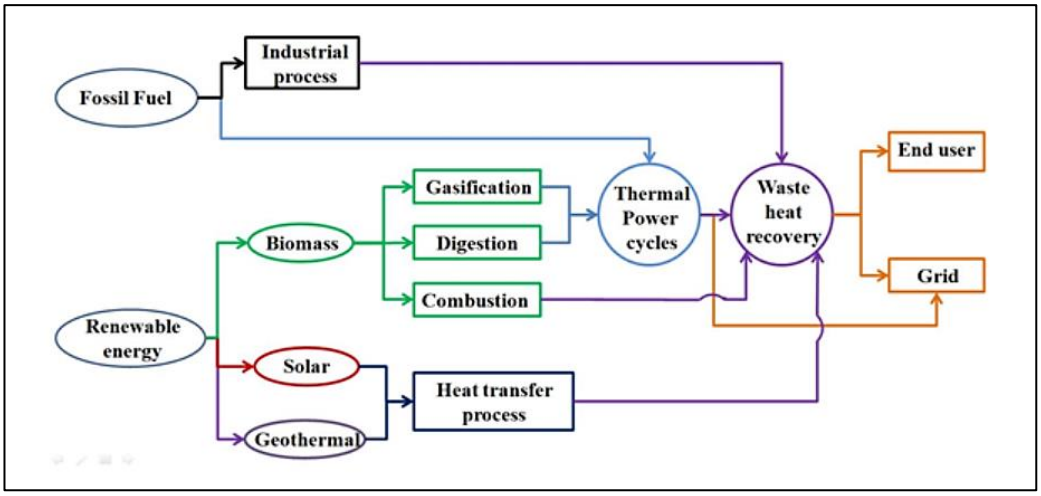

Figure 1.4. Waste heat recovery from various heat sources.

The obstacles to the widespread adoption of recovery technology for low-temperature waste heat have been outlined as follows to realize an affordable and effective waste heat recovery process: (1) The inconsistency of waste heat sources, (2) the mismatch between user demand and energy grade of the waste heat resource in terms of time and space, and (3) the absence of a thorough methodology for system-level global energy transfer and transformation optimization, particularly for larger zones[10].

1.3. MODERN THERMODYNAMIC CYCLES FOR RECOVERING WASTE HEAT

Regarding the caliber of waste heat sources, several implementation strategies can be used. The fundamental strategy is to drive the thermodynamic cycle and transform thermal energy into useful electricity by using the available waste heat as a source of heat. Among the most crucial the operation temperature is one of the criteria for selecting a suitable cycle. Figure (5) depicts the possible thermodynamic cycles and the range of their relevant operation temperatures [11]. The Steam Rankine Cycle (SRC) is best suited for medium-high temperature waste heat, which is more than 300 °C. The cost-effectiveness of systems for lower-temperature heat sources is significantly lower, and they run the risk of causing surface corrosion issues. Additionally, the Organic Rankine Cycle (ORC), which employs organic fluids with lower boiling points, has also been thoroughly studied in recent years. The ORC can operate at competitive efficiency when the waste heat is between 90 and 250 degrees Celsius. Additionally, to closely match the temperature profile of waste heat sources throughout the phase change heat transfer process, between 100 °C and 450 °C, the Kalina Cycle uses a mixture of ammonia and water as the working fluid.

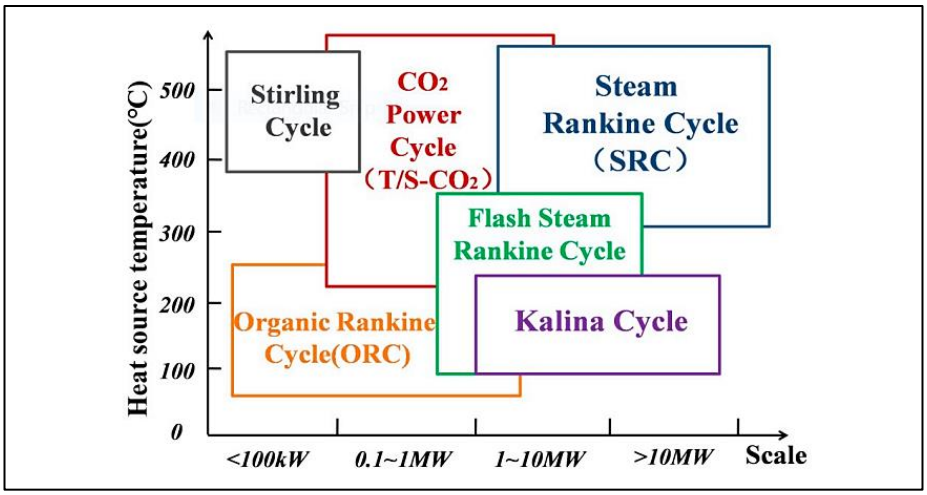

Figure 1.5. Thermodynamic cycles for waste heat recovery at different temperature ranges and scales.

The utilization of CO_2 power cycles for waste heat recovery has received more and more attention in recent years. Due to carbon dioxide's relatively low critical point,

such cycles are often run in trans-critical or supercritical conditions. These key benefits can be summed up as follows.

First off, unlike the steam-based Rankine cycle, which is only effective for recovering waste heat at high temperatures, CO_2 cycles are ideal for recovering waste heat from sources with a wide range of temperatures. Therefore, the primary reason for looking into CO_2 power cycles was not only to replace the SRC [11], but also to provide a wider range of temperatures for waste heat recovery [12]. Additionally, the non-combustible and non-toxic nature of CO_2 allows for additional room for the cycle operation temperature to rise. In addition, the CO_2 power cycles occupy a smaller space as compared with SRC, which has a large working fluid steam volume and therefore shows great potential for system downsizing and is lightweight. Accordingly, the chemistry and condensing processes are also simpler [13].

In summary, supercritical carbon dioxide (s-CO_2) cycles offer a wide range of operating temperatures, potentially higher efficiency, and a substantially smaller environmental footprint than typical thermodynamic cycles [14][15]. The number of articles has increased significantly in recent years as a result of the widespread interest in power cycles fueled by s-CO_2. This comprehensive assessment of recent developments in s-CO_2 cycles for waste heat recovery is extremely pertinent because the technology's enormous potential in waste heat recovery has to be further investigated.

1.4. s-CO_2 POWER CYCLE IMPROVEMENTS FOR WASTE HEAT RECOVERY

Based on the order of energy use, a cogeneration system may often be divided into a topping- and a bottoming cycle. While in a bottoming cycle waste heat from a topping cycle is further used to generate power through a recovery heat exchanger and a turbine machine, in a topping cycle the input primary energy is used to first produce power and thermal energy. Bottoming cycles are appropriate for recovering low-grade waste heat generated by industrial operations to achieve cascade energy utilization.

The use of carbon dioxide as a working flow operating at supercritical parameters instead of water is a promising way to increase thermal efficiency and reduce the cost of power plants allowing the implementation of the Brayton Cycle at low costs for auxiliary needs at a moderate initial temperature and compact dimensions of the main power equipment [16]. The reasons why researchers around the world are interested in this technology are largely related to the advantages of carbon dioxide in comparison with other heat carriers such as water. In particular, carbon dioxide heat carriers feature low values of critical temperature (30.98 ◦C) and pressure (7.38 MPa) While water has a relatively high critical temperature (374.10 ◦C) and pressure (22,064 MPa) as shown in Figure (6).

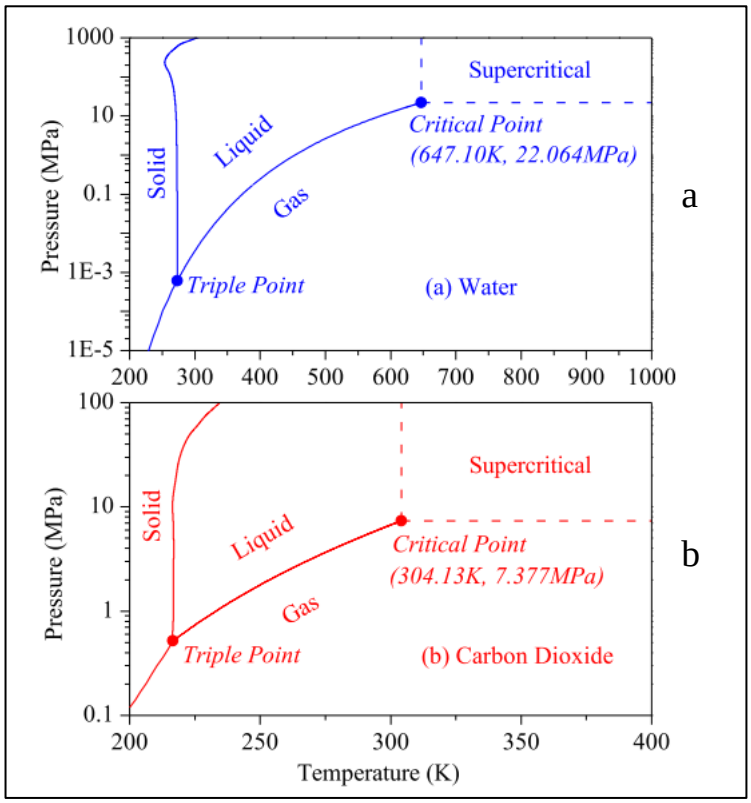

Figure 1.6. The three-phase pattern for water and CO_2 (a: water, b: CO_2).

The low critical temperature of carbon dioxide, being close to the ambient temperature, makes it possible to compress the working flow near the saturation line [17], which reduces the compressor workload and the temperature of heat removal from the cycle without condensation of the working flow. In addition, carbon dioxide has a relatively low aggressiveness as compared to water and shows its corrosive activity only in the

presence of moisture in gas or a water film on the metal surface. The price of carbon dioxide gas is comparable to that of the water heat carrier.

1.5. CONFIGURATIONS OF SCO2 BRAYTON CYCLES

Long-term thermodynamic studies of S-CO_2 power facilities resulted in the development of the five cycles presented in Figure (7) [18].

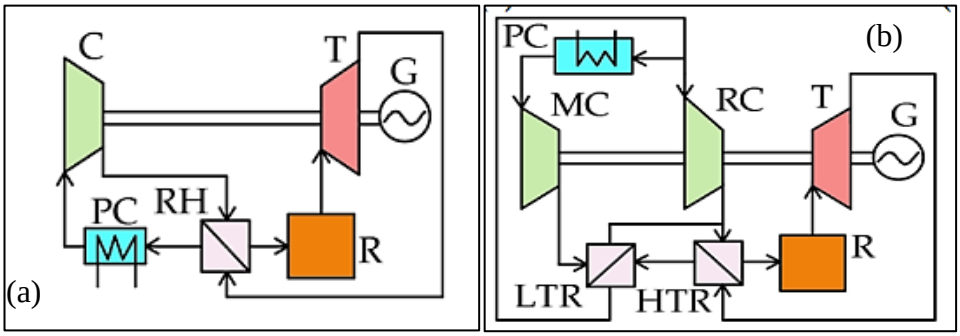

Figure 1.7. Supercritical CO_2 Brayton cycles: (a) S-CO_2 Brayton cycle with recuperator (b) S-CO_2 Brayton cycle with recompression.

A SCO2 simple recuperator Brayton cycle (SRBC), as depicted in Fig. 7(a), is proposed to increase the SCBC's overall thermal efficiency by recovering heat from the recuperator. However, the high-pressure side of the recuperator has a higher CO_2 heat capacity than the low-pressure side, and this might result in low efficiency due to an internal "pinch point" that exists.

As shown in Fig. 7(b), a SCO2 recompression Brayton cycle (RCBC) The flow is split into two streams before cooling, with one going to the recompression compressor and the other passing through the chiller to the main compressor. The flow that passes through the low-temperature recuperator should be mixed with another stream at the same pressure and temperature. The low mass flow at the high-pressure side of the low-temperature recuperator prevents the pinch point issue, making the heat capacity mass flow weighted on both sides equal. This system rejects less heat, and thermal efficiency is increased since the re-compressor's input effort is less than the heat saved[19].

1.6. THE ENERGY SITUATION IN IRAQ

Iraq's electricity production has currently reached 26 Giga Watts, the highest in its history, and although it has reached this limit, it still has not reached self-sufficiency, which amounts to 37 Giga Watts, according to statistics from the Iraqi Ministry of electricity for the year 2023, Iraq needs to add 11 Giga Watts to its production.

Due to the rapid population growth and Urban Development, Iraq needs to raise its electricity production annually by 6-8%, equivalent to 2000-3000 megawatts. Iraq relies mainly on fossil fuels (oil and gas) for electricity production, according to eia statistics as shown in the figure (8) [20].

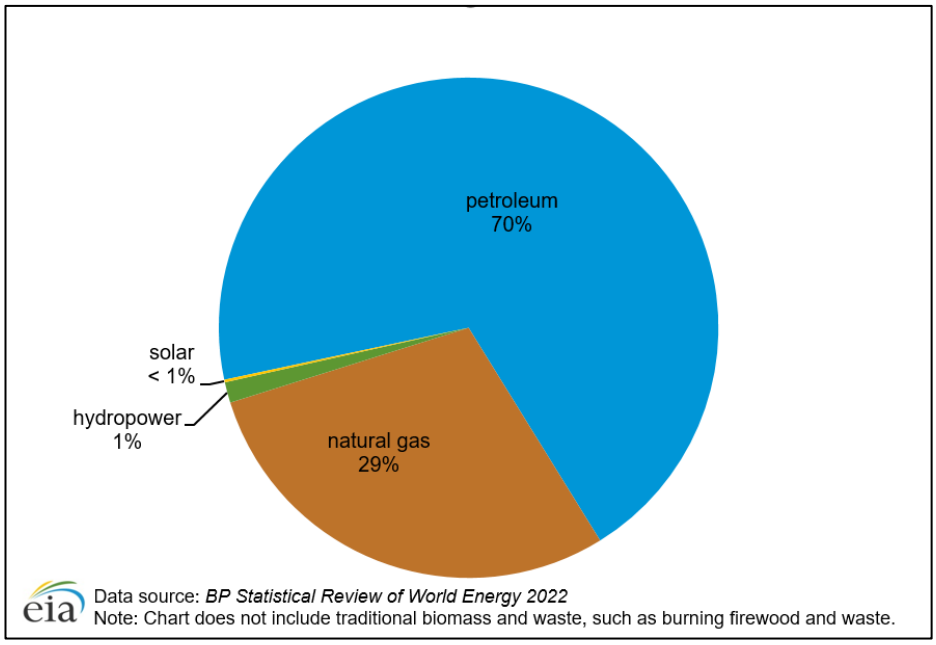

Figure 1.8. Iraq's total primary energy consumption.

Iraq's electricity is produced through 79 generating stations distributed in all Iraqi cities, almost 40% of the stations are gas turbine stations and there are plans to put 8 stations into service by 2024-2025, as the Iraqi government contracted with Siemens to develop and increase the efficiency of gas stations and the construction of new stations, among these aspirations is the addition of steam stations to gas stations.

1.7. CURRENT STUDY

In this current study, we will simulate a combined cycle power plant where the upper cycle is the gas Bryton cycle and the bottoming cycle is the supercritical carbon dioxide cycle to take advantage of the waste heat from the exhaust gases and raise the overall efficiency of the station.

We will calculate the wasted energy of one of the stations located in Iraq, make an energy and Exergy analysis of all parts of the Bottom station, and indicate the additional energy produced to the electricity grid.

In addition, this study examines the possibility of applying these courses in all gas stations in Iraq as it is less expensive than the Steam Rankine cycle, the smallest area, and the fastest application.

PART 2

LITERATURE REVIEW

In 1968, Feher et al. examined the attributes and benefits of supercritical cycles. The researchers discovered that the supercritical cycle provides excellent thermal efficiency, a low ratio of volume to power, no erosion of the turbine blades, no cavitation in the pump, a turbine and pump with just one stage, a heat rejection process using a single-phase fluid, and is not affected by compression efficiency.

Furthermore, they deliberated that using carbon dioxide as the operational substance and a nuclear reactor as the heat supplier enables the supercritical engine to function as a little, transportable electric power generator [21].

In 2004, Dostal et al. conducted an assessment of the supercritical carbon dioxide (sCO_2) power cycles specifically for nuclear applications. The turbine input temperature was cautiously chosen to be 550 degrees Celsius, while the compressor output pressure was set at 20 megapascals. Under these specific operating circumstances, the direct cycle achieves a thermal efficiency of 45.3% and lowers the cost of the power plant by about 18% when compared to a traditional Rankine steam cycle. The present operational experience of the reactor involves using CO_2 at temperatures reaching up to 650 °C. This temperature is used as the input temperature for the advanced turbine design. The improved design exhibits a thermal efficiency of around 50%. Additionally, the reactor system using the direct supercritical CO_2 cycle is approximately 24% more cost-effective than the steam indirect cycle, and approximately 7% more cost-effective than a helium direct Brayton cycle. The turbomachinery is very small and reaches an efficiency of over 90%. The turbine body of the 600 MW/246 MW power plant has a diameter of 1.2 m and a length of 0.55 m, resulting in a very high-power density of 395 MW/m3. The compressors are more compact due to their operation near the critical point, resulting in a larger fluid density

compared to the turbine. The power conversion unit, which contains these components plus the generator, has dimensions of 18 meters in height and 7.6 meters in diameter. The power density of this substance is about 46% more than that of helium [22].

In 2008, Shintaro et al. conducted research comparing the fundamental properties of cycle efficiency feasible in steam turbines, helium turbines, and carbon dioxide turbines, without any limitations on the heat source. The prototype nuclear fusion reactor is evaluating power generating methods, including the steam turbine cycle, helium turbine cycle, and supercritical CO_2 (S-CO_2) turbine cycle. Their attainable cycle thermal efficiencies are determined to be 40%, 34%, and 42% at the heat source output coolant temperature of 480 °C, respectively, in the absence of any additional limitations. Currently, the system incorporates a low-temperature diverter heat source. The steam turbine system and the S-CO_2 turbine system were evaluated in terms of cycle efficiency and plant cost in this specific situation. The steam cycle had a cycle efficiency of 37.7%, whereas the S-CO_2 cycle showed a cycle efficiency of 36.4%. The building cost was calculated using the method of component volume. The capacity of the steam turbine system is 16,590 m^3, whereas the volume of the S-CO_2 turbine system is 7,240 m^3. Furthermore, the process of isolating tritium that has infiltrated from the coolant is much simpler in S-CO_2 compared to H_2O. Thus, the S-CO_2 turbine system is preferable to the steam turbine system for the fusion reactor system [23].

In 2010, Sandia and others conducted a study on supercritical carbon dioxide (sCO_2) as a potential energy carrier for solar, nuclear, or fossil fuel-based heat sources. This study has primarily focused on the supercritical CO_2 cycle (S-CO_2), which has the potential to achieve high efficiency within the desired temperature range for both heat sources. Additionally, the S-CO_2 cycle is very compact, hence offering the possibility of reduced capital expenditures. The first phase in the development of these sophisticated cycles was the creation of a compact Brayton cycle loop.

Approximately 100 test operations have been conducted on the loop, including evaluations of the compressor performance map, thrust loads (with just a compressor or with a tiny turbine), testing on labyrinth seal leakage, operations in the two-phase

area, and utilization of gas foil bearings. The loop has been operated at speeds of up to 65,000 rpm, flow rates of 4 lb/s, and a pressure ratio of 1.65 [24].

in 2011 Turchi et al. conducted a study on supercritical carbon dioxide (sCO_2) power cycles for their use in concentrated solar power (CSP) facilities. Initial investigation indicates that the fluid may be more suitable for use in Power Towers. The task of circulating high-pressure supercritical carbon dioxide ($S\text{-}CO_2$) through a sizable Power Tower would pose difficulties given the substantial volume and pressure of the fluid being transported. Nevertheless, this research presents a modular power tower design that may use the potential of $S\text{-}CO_2$ without incurring excessive expenses for pipes. The suggested concept simplifies the power system configuration by using a single-phase process that employs $S\text{-}CO_2$ as both the heat transfer fluid (HTF) and the thermal power cycle fluid. The architecture is suitable for thermal energy storage that involves the storage of sensible heat. The $S\text{-}CO_2$ process's streamlined gear and small size may help decrease the expenses associated with installing, maintaining, and operating the system. Brayton-cycle systems using $S\text{-}CO_2$ exhibit reduced weight and volume, decreased thermal mass, and simplified power blocks in comparison to Rankine cycles. This is attributed to the greater density of the fluid and the more straightforward design of the cycle. The reduced thermal mass enables quicker startup and load adjustment for frequent startup/shutdown operations and load adaptation compared to a system based on high-temperature fluid (HTF) or steam. The study aims to analyze and assess the performance of an advanced $S\text{-}CO_2$ Brayton cycle power production system in conjunction with a modular power tower CSP system[25].

In 2012, Pasch et al. constructed a sCO_2 test loop. The main elements of the finalized technical apparatus consist of two turboalternator compressors with their respective motor/controllers, three printed circuit heat exchangers, and six shell-and-tube heaters with their corresponding controllers. The main components that assist are a cooling tower, a load bank that dissipates power, and equipment for managing leakage flow. Upon achieving this milestone, we expect a substantial rise in CBC R&D efforts, aiming to enhance the technical readiness level of components that are now seen as underdeveloped by the industry. In addition, they provide comprehensive explanations

of the various components and operating software required to run the recompression CBC [26].

In 2013, Allam et al. successfully developed a system that utilizes hydrocarbon fuels and effectively absorbs 100% of air emissions, including all carbon dioxide. This is done by a closed-loop, high-pressure, low-pressure-ratio recuperated Brayton cycle that uses supercritical CO_2 as the working fluid. The cycle capitalizes on the unique thermodynamic characteristics of carbon dioxide as a working fluid, thereby mitigating the energy losses inherent in steam-based cycles caused by the heat required for vaporization and condensation. The system's strong economic performance is due to its high target efficiencies of 59% net LHV for natural gas and 51% net LHV for coal. This is achieved by using a single turbine, which reduces the plant's size and the number of components required. As a result, the system has lower projected capital and O&M costs compared to similar fossil-fuel systems [27].

In 2013, Le Moullec et al. conducted a study to determine the practicality of implementing a coal-fired power plant using a supercritical carbon dioxide (sCO_2) cycle. A coal power station using a CO_2 power cycle, but without carbon capture, has the potential to attain a net efficiency of 50% (LHV) while operating at a maximum temperature and pressure of 620 °C and 300 bar. These performance figures have yet to be confirmed, but the first findings from the pilot plant are promising. The CO_2 capture method uses monoethanolamine as a solvent and is fitted with vapor recompression units to minimize the heat needed from the CO_2 cycle. The particular boiler duty of the system is about 2.2 GJ per tonne of CO_2, whereas the electrical auxiliary usage, including compression to 110 bar, amounts to 145 kWh per tonne of CO_2. The assessment of the power plant's energy output emphasizes the favorable prospects of using a CO_2 supercritical cycle. An attainable net power plant efficiency of 41.3% (LHV) may be achieved by using existing or almost existing equipment, together with carbon collection and compression of CO_2 to 110 bar. A comprehensive technical and economic assessment of the planned power plant has been conducted. The data indicates a 15% decrease in the levelized cost of energy and a 45% reduction in the cost of avoiding CO_2 emissions, excluding transportation and storage. This is in

comparison to a typical carbon capture technique used in a reference supercritical coal-fired power station [28].

in 2015 KIER designed the turbomachinery used in sCO_2 power cycles. A 10-kilowatt electric power class experimental loop was created, which utilizes a turbo-alternator-compressor unit. The unit consists of a centrifugal compressor and a radial turbine, operating with supercritical carbon dioxide in a basic unrecuperated Brayton cycle. An enclosed design of a compressor impeller and a turbine wheel with labyrinth seals were developed to counteract thrust. Addressing the issues related to the equilibrium of the high-pressure fluid turbomachinery. Furthermore, this particular kind does not encounter any problems related to thermal expansion, collisions, or lack of clearance between a shroud and a wheel. The first procedure, conducted at a speed of 30,000 revolutions per minute, a turbine inlet temperature of 83 °C, and a pressure of 8500 kilopascals, was accomplished. It has been determined that all stages of the cycle were present in the supercritical area [29].

In 2015, Ricardo et al. conducted a thorough study of energy using four different configurations of the S-CO_2 Brayton cycle. These configurations include the tiny Brayton cycle, Brayton Cycle Recompression, Partial Cooling with Recompression, and Recompression with major intercooling. They may be manufactured with or without the process of reheating. Cooling is used in Brayton supercritical cycles and solar receivers as a substitute for the heater and reheater found in traditional Brayton cycles. This allows for a reduced introduction of heat into the cycles. In this research, a dry air cooler is used before the compressor input for all supercritical Brayton cycles under investigation. In standard Brayton cycles, a solar receiver is used as a substitute for the heater and reheater to provide heat to the cycles. An analysis was conducted on the impact of turbine intake temperature and cycle design on thermal performance and exergy destruction. The findings demonstrated a consistent and continuous improvement in the thermal efficiency of the supercritical CO_2 Brayton cycle as the cycle's temperature rises. The recompression cycle, with main compression intercooling, demonstrated the highest thermal efficiency (gI = 55.2% @ 850 °C). The comprehensive exergy study revealed that the solar receiver is responsible for the majority of exergy destruction, accounting for over 68% of the total. In contrast, the

turbines and compressors make only a small contribution, accounting for less than 3% collectively. Additionally, it is observed that the effectiveness of exercise follows a bell-shaped curve, peaking at a maximum value between 700-750 °C, depending on the design of the cycle [30].

In 2015, Hanzhen et al. conducted a selection and verification process for S-CO_2 turbine types and rotational speeds, specifically for power outputs of 15 MW and 1.5 MW. The turbine type for a power output of 15MW is axial, whereas for a power output of 1.5 MW, it is radial. An empirical study was carried out to examine the aerodynamics, technical design, and overall performance estimation of several SCO2 turbines. The specific characteristics of SCO_2 are obtained as inputs for the model from the Refprop database, which is supplied by the US National Institute of Standards and Technology (NIST). The commercial CFD program - NUMECA - is used to conduct a comprehensive aerodynamic study. This analysis is based on a complete 3D model of the nozzle vane pathways and rotor flow field. Furthermore, the study of turbine force is conducted using the commercial program ANSYS / Mechanical, while considering the impact of the pressure load exerted by the working fluid [31].

in 2016 Weiland et al. conducted a study on the conceptual design of direct-fired sCO_2 plants. This research presents a fundamental configuration of a coal-fired cycle, in which coal is first converted into gas and purified to prevent the introduction of sulfur and particulate matter into the sCO_2 cycle. The sCO_2 cycle's oxy-combustor operates using syngas. The first design of the sCO_2 plant achieves a net thermal efficiency of 37.7% (HHV), while capturing 98.1% of CO_2 at a purity level of 99.4%. When compared to the reference IGCC plant, this plant demonstrates a higher level of performance. It achieves a net HHV thermal efficiency of 31.2% and a CO_2 capture rate of 90.1% at a purity level of 99.99%. The article examines the impact of process factors on the performance of the sCO_2 plant, as well as their influence on the plant's operability and cost surrogate variables [32].

In 2017, Zhu et al. substituted the heater and reheater with a solar receiver exclusively designed to provide heat for S-CO_2 cycles. Furthermore, their research primarily focuses on analyzing the thermodynamic efficiencies of different S-CO_2 cycles

individually, without assessing the total efficiencies of SPT systems that include directly heated S-CO_2 cycles. The findings demonstrate that the TIT (Turbine Inlet Temperature) has a parabolic impact on the overall efficiencies of each S-CO_2 (Supercritical Carbon Dioxide) cycle. Among the different cycles, the intercooling S-CO_2 cycle achieves the highest overall efficiencies, followed by the recompression, partial-cooling, pre-compression, and simple cycles, at varying TIT values. In addition, the partial-cooling cycle has the highest overall specific work at each TIT and provides higher overall efficiencies compared to the recompression cycle at a constant TIT of 650 °C. This is because the UAtotal value is relatively low, which has the potential to lower the costs of integrated SPT systems with limited UAtotal values [33].

In 2017, KIER designed and analyzed a 10 kilowatt electric (kW_e) supercritical carbon dioxide (sCO_2) test loop. Sub-kilowatt class test loops were built, one with a high-speed radial type turbo-generator and another with an axial type turbo-generator capable of generating tens of kilowatts. To address the technological limitation of S-CO_2 turbomachinery, the implementation of a partial admission nozzle and oil-lubrication bearings was used in the turbogenerators. To explore the closed-power cycle and establish an effective operational plan for a high-pressure S-CO_2 system, an experimental test was conducted using an organic Rankine cycle (ORC) with a refrigerant as the working fluid. The choice of refrigerant was based on its ability to operate under relatively low-pressure conditions, typically around 30 to 40 bar. The sub-kW_e class test loop was used using R134a as the working fluid, resulting in an average turbine output of 400 W [34].

In 2018, KIER developed and produced a supercritical carbon dioxide (sCO_2) test loop equipped with an axial turbo generator to resolve the problem related to turbomachinery. A 4.5-kilowatt electric generator, designed using a radial-type turbo-generator, a labyrinth seal, and an angular contact ball bearing, was created to operate a straightforward recuperated trans critical cycle. An 86 MW of electrical power was generated over 30 minutes with a turbine inlet condition of 320 °C. Furthermore, a 60-kilowatt electric power generator was created, using a single-stage axial impulse-type turbo-generator. This turbo-generator has a typical carbon floating ring seal and oil-

lubricated tilting bearings. A power output of 10 kilowatts was achieved for 4.2 hours by using a liquid CO_2 pump in a simple trans critical cycle. The turbine intake was maintained at a temperature of 212 °C and a pressure of 123 bar. A continuous closed loop was effectively operated by including a leakage make-up loop. Furthermore, there is now ongoing development of a twin Brayton test loop with a power output of 120 kilowatts electric (kW_e), designed to operate at turbine inlet conditions of 500 °C and 130 bar. The development of a flue-gas heater, a centrifugal compressor with a dry gas seal, and two recuperators was undertaken [35].

In 2018, Kun et al. conducted a comprehensive analysis to compare the performance of the S-CO_2 Brayton cycle with various designs. The study focused on making multi-objective enhancements for SPT stations using different S-CO_2 Brayton CY systems. The findings indicate that the inter-cooling cycle layout and the partial-cooling cycle layout generally achieve the highest level of performance, followed by the recompression cycle layout and the pre-compression cycle layout. Conversely, the simple recuperation cycle layout exhibits the lowest level of performance. The partial cooling cycle pattern and the inter-cooling cycle layout provide more noticeable benefits compared to other cycle configurations when dealing with high compressor intake temp[36].

In 2019, Alsagri et al. conducted an analysis of the thermodynamic and economic aspects of sCO_2 cycles for their use in CSP facilities. The goals were to evaluate the feasibility of the system in a location with ample solar energy at moderate to high temperatures during the day and to examine the impact of thermal energy storage with varying durations (4, 8, 12, and 16 hours) on increasing the proportion of solar energy used and the overall annual energy production capacity. To maximize energy output while minimizing costs, the design of the heliostat geometry field is combined with a sCO_2 Brayton cycle and a molten salt thermal energy storage (TES) dispatch system. The related operational parameters are then optimized the research findings indicate that SPT-TES with a supercritical CO_2 power cycle is economically viable with 12 hours of thermal storage using molten salt. The results also show that integrating 12 hours-TES with an SPT has a high positive impact on the capacity factor of 60% at the optimum LCOE of $0.1078/kWh [37].

In 2019, Cho et al. enhanced the efficiency of an S-CO_2 Brayton cycle by enhancing the aerodynamic performance of an S-CO_2 centrifugal compressor. They investigated the impact of altering the backward sweep angle at the impeller exit to determine if the previously determined optimal backward sweep angle for an air centrifugal compressor is still applicable when the fluid is different. The research indicates that an S-CO_2 centrifugal compressor may attain maximum efficiency at a back sweep angle of 700, above the usual design value. Additionally, it has been shown that the change in compressibility factor does not affect the overall efficiency of the system, since its Mach number remains below one. According to the findings, a backward sweep impeller may get a greater pressure ratio and maintain stable operation over a larger range when the mass flow rate is reduced [37].

In 2019, Bennett et al. conducted a study to examine the potential use of sCO_2 cycles for load balancing in a dynamic grid that is mostly powered by renewable energy sources. This research used a collection of precise and detailed generation and demand data, as well as advanced forecasting capabilities, specifically designed for the microgrid at the University of Virginia. The findings indicate that when solar power is extensively used, sCO_2 cycles and steam combined cycle systems with ramp rates above 5.75% per minute may effectively manage the power demand and provide similar levelized prices of energy at $0.057 per kilowatt-hour. The minimal part load capacities were the cause of solar curtailment. The analysis projected that a supercritical carbon dioxide (sCO_2) cycle, which operates at a minimum part load of 30%, would experience a reduction in output of 15% in a high solar scenario when no battery is used. However, when a 30MWh battery is used, the reduction in output is reduced to 4% [38].

In 2019, Astolfi, M. et al. The study specifically examined the feasibility of using a closed-cycle system with supercritical carbon dioxide to recover waste heat. The objective of this work is to close the distance between the first numerical investigations and the development of actual power systems. The results indicate that sCO_2 recuperative cycles when fitted with a CO_2 storage tank, exhibit a consistently high efficiency, which remains almost constant until the normalized flue gases mass flow rate reaches 50%. However, constant inventory systems are projected to have a lower

efficiency. Both systems may be run at a load as low as 30% without causing any issues to the system components. Additionally, the minimum plant efficiency of both solutions remains competitive when compared to ORC technology. Optimal performance is achieved by actively regulating the cycle inventory to optimize both the lowest pressure and maximum temperature at each part-load situation [39].

Alfani, D. in 2019. The authors conducted a review that presents new insights into the design and selection of heat exchangers and materials. These insights were gained during the construction of a 50 kW sCO_2 testing facility for waste heat recovery (WHR) applications. Additionally, the authors highlight the advantages of using CO_2 as a working fluid in heat-to-power conversion systems, including improved efficiency, compactness, and operational flexibility compared to conventional technologies. Although there has been much study conducted in the sector, the technical readiness level remains relatively low. The resultant map offers valuable information for the first selection of the most appropriate heat-to-power conversion technology for a certain industrial waste heat stream [40].

In 2020, Gkountas et al. conducted a study in which they utilized an aqueous nanofluid as the coolant for the precooler of a S-CO_2 Brayton cycle. Specifically, they employed an Al_2O_3-water nanofluid. The researchers examined how the performance of a Printed Circuit Heat Exchanger (PCHE) is improved by using this nanofluid. Additionally, they investigated how the thermophysical properties of the nanofluid impact the enhancement of heat transfer, specifically in terms of the size of the heat exchanger, while keeping the flow rate and heat transfer constant. The findings indicate that using a nanoparticle volume fraction of 5%, the highest value used in this study led to a 10% enhancement in the heat transfer coefficient compared to the working fluid consisting only of pure water. As a result of this enhancement, the overall length of the heat exchanger was reduced by 0.9%, and the pressure drops were reduced by up to 14%. The analytical computations are expected to be very beneficial due to the advancing research in the nanofluids sector [41].

In 2020, Yang et al. conducted a study on the part-load performance of four common S-CO_2 Brayton cycles: the simple recuperative cycle, the reheating cycle, the

recompression cycle, and the intercooler cycle. They also investigated the impact of three common improvement methods (reheating, recompression, and intercooling) on the cycle performance under part-load conditions. The results indicate that the reheating cycle exhibits superior efficiency compared to the basic recuperative cycle. Additionally, the recompression cycle and intercooling cycle outperform the reheating cycle in situations when the load is not at maximum capacity. Nevertheless, the intercooling cycle demonstrates superior efficiency compared to the recompression cycle alone when the load is above 60%. The decline in efficiency of the reheating cycle is negligible as the load lowers. This cycle exhibits the most optimal response to the need for a broad range of load modifications. The recompression cycle exhibits superior performance when the ratio of the actual total power production to the maximum total electricity output in a given time is below 62.5%. When the ratio exceeds 68.3%, the intercooling cycle exhibits superior performance. Overall, the intercooling cycle does not exhibit a substantial improvement in efficiency relative to the recompression cycle when operating under load-following circumstances [42].

In 2021, Sleiti et al. conducted a study where they examined and compared the efficiency of five new configurations for CO_2 power cycles. They developed detailed models to analyze the energy and exergy of these configurations, considering factors such as the amount of water vapor present and the changes in specific heat of sCO_2. The study also investigated the impact of key operating parameters, including pressure ratio, intermediate pressure ratio, turbine inlet temperature, and compressor inlet temperature. Additionally, the researchers examined the performance of these configurations under moderate turbine inlet temperatures ranging from 550 °C to 750 °C. The findings indicate that the partial intercooling cycle (PIC) outperforms other setups at higher turbine inlet temperature (TIT) and lower pressure ratio (PRR). The PIC achieves a maximum thermal efficiency of 52% when the RC is set to 5, RPR is set to 0.45, TIT is set to 750 °C, high pressure is set to 20 MPa, and CIT is set to 50 °C. In addition, the reheating cycle has the best second law efficiency, but with just a little boost in thermal efficiency compared to the dual recuperator cycle (DRC) [14].
In 2021, Uusitalo et al. conducted a study to examine whether radial turbine designs driven by CO_2 and with varying specific speeds adhere to the established efficiency graphs derived from ideal gas turbines. Additionally, they investigated the impact of

design power scale and specific speed on radial inflow turbines operating with supercritical CO_2 in the power range of 0.1 MW_e to 3.5 MW_e. The findings indicate that both the specific speed and mass flow rate significantly influence the turbine's The turbine designs that exhibited the best isentropic efficiencies were found to have specific speeds ranging from 0.50 to 0.60. For turbine power outputs ranging from 100 kW to a few hundred kW, the most important loss is due to tip clearance. However, at higher power levels, the most significant causes of loss are the passage, stator, and exit kinetic losses [43].

In 2021, Shiyi et al. conducted a thermodynamic assessment of the oxygen-fuel combustion process in conjunction with the carbon dioxide cycle. They used a well-documented technique and reasonable industrial assumptions, taking into account materials that are now in use and considering a very near future timeframe. The plant is enhanced by the use of heat recovery from the flue gas and the implementation of an Air Separation Unit (ASU) to optimize both the electrical efficiency and the heating efficiency. A comparison was made between distinct flue gas recycling modes, namely wet mode and dry mode, for oxy-fuel combustion. At the specified conditions of 30 MPa/600 °C / 600 °C, the electrical efficiencies for the wet and dry modes were 36.6% and 35.3% respectively. The heating efficiencies for the wet and dry modes were 15.4% and 14.9% respectively. The total efficiency for the wet mode was 52.0% and for the dry mode was 50.2%. In addition, the rate of CO_2 collection was found to be around 99.94%. The residual heat from the air separation unit and the flue gas was captured and combined with the sCO_2 cycle. It was observed that this heat recovery reduced the split ratio for recompression and resulted in an increase of 0.3-2.7 percentage points in electrical efficiency, as well as an increase of 0.3-2.1 percentage points in heating efficiency [44].

In 2021, Mengchao et al. introduced a novel approach to creating these cycles by incorporating computational intelligence into the realm of thermodynamics. He demonstrated a comprehensive model of the cycle, which involved simplifying and coding the cycle, as well as designing a two-layer optimization algorithm. The upper algorithm focused on cycle generation, while the lower algorithm focused on optimization. Additionally, the course covered the design of the basic configuration

and heat exchange network, with the study of accuracy in algorithms being explored through three cases [45].

In 2021 Alfani, D. et al. conducted primarily examined the performance and control techniques of a supercritical carbon dioxide (sCO_2) cycle utilized as a power cycle. This cycle utilizes a heat source derived from a flue gas stream generated by a waste heat recovery process. This study explores various operational approaches to optimize the configuration of a recuperative recompressed cycle. It considers different combinations of component features, including (1) turbine and compressor (with fixed or variable velocity, with or without variable geometry), (2) heat rejection unit (with fixed or variable fan speed), and (3) fluid inventory (variable or fixed). The findings indicate that the highest total recovery efficiency achieved was 22.65%. This was attained by operating at a maximum cycle temperature of 346.7 °C and a maximum pressure of 181.3 bar while maintaining a minimum pressure of 81.1 bar [46].

In 2022, Gotelip et al. introduced an optimization process that includes the boundary conditions of a given use case. They examined several sCO_2 cycle topologies and reported the findings of the optimal cycle architecture and fluid parameters. The objective was to maximize heat recovery while minimizing expenses. The findings indicate that the Dual Rail e SDR architectural design yielded a net power increase of about 5% compared to the Sequential Heating method, a 32% increase compared to the Regenerative cycle, and a remarkable 79% improvement compared to the Simple cycle. The Sequential Heating design has the greatest capability for harnessing the assessed heat source. This design yields NPV results within the region of 16 million dollars, surpassing the more intricate systems by around 19% and also achieving 3% lower LCOE values. In addition, the design improves the Regenerative cycle by 54% in terms of NPV and achieves a 20% increase in net power. The findings indicate the ideal operating settings unique to each layout that promote the optimum balance between thermal and economic performance. In architecture, the best outcomes are often reached within a range of 90% to 93% of the maximum power attained by the arrangement. The findings demonstrate a significant capacity for the suggested cycle structure and operating circumstances for recovering exhaust heat in a combined gas turbine sCO_2 cycle cle [47].

In 2022, Saboora et al. created a software package to accurately determine the key factors that affect the central receiver system. This includes the detailed design of the heliostat field pattern, angles that define its characteristics, optical efficiency, and thermal energy storage. The software is also capable of analyzing two different configurations of the Brayton cycle. The impact of seasons on the operational efficiency of solar power plants is analyzed by examining variations in net power output and cycle efficiency based on daily meteorological data under various climatic circumstances. The suggested devices function continuously for 24 hours, with a heat transfer fluid moving in a sinusoidal pattern between the solar receiver and storage tanks. The results indicate that the linked system operates more efficiently while using the recompression cycle design, with a fluctuation range of 39% to 45%. The calculated average net power production is 37.17 MW and 39.04 MW for the regeneration and recompression cycles, respectively. The comprehensive methodology that was created and the calculated findings obtained are very significant for the future implementation of the supercritical carbon dioxide Brayton cycle in concentrated solar power plants[48].

In 2022, Zhiyuan et al. analyzed the efficiency and cost-effectiveness of the supercritical CO_2 Brayton cycle. This analysis was based on dynamic component models and constraint circumstances. The specified parametric limitations for the compressor are as follows: the range of compressor input temperature is from 305 K to 310 K, the range of inlet pressure is from 7.4 MPa to 8.3 MPa, and the range of maximum cycle pressure is from 15 MPa to 30 MPa. The findings demonstrate that the attainable efficiency of a basic cycle is 0.13e0.62% points below the theoretical maximum efficiency, taking into account restriction circumstances. Under constrained circumstances, the levelized cost of energy (LCOE) is 0.00038e0.00085$/(kW$h) more than the theoretical minimal LCOE. In a recompression cycle, constraint circumstances have a more substantial influence. The cycle's efficiency is reduced by 0.81e1.21% due to restrictions, resulting in a lower practical efficiency compared to the maximum efficiency. Similarly, the LCOE (Levelized Cost of Electricity) under constraint circumstances is higher by 0.0012e0.0018$/(kW$h) than the theoretical minimum LCOE [19].

2.1. NOVELTY

Previous research has focused on the correct employment of supercritical carbon dioxide power plants, comparing the types of cycles available such as simple, recompression, and reheating, Besides testing different sources of heat such as solar, nuclear, fuel cells and recovering waste heat energy factories and generating plants and making them function separately or in combination, as well as calculating the economic feasibility of using these stations according to regular standards, and environmental validation that will result from the use of this type of station. In our present study, it has been proposed to add a recompressed recuperative Sco2 Brayton power plant to a Brayton gas power plant in Hilla, Iraq to take advantage of the exhaust heat energy and to reduce the shortage of electricity production. We will undertake energy, exergy, economic, and environmental analysis and take into account the effect of the total and partial loading of the main station.

PART 3

MATERIALS AND METHODS

In the present study, first, the followings are points to be determined:

- Waste gas resources and properties such as:
  - Temperature
  - Mass flow rate
- Type of power plant and its production capacity.
- Choosing a heat transfer method.
- Achieve simulation of the added Station by using the Anaconda program (Python).

As we have already mentioned, supercritical carbon dioxide plants are a promising option for generating electric energy by taking advantage of the waste heat from various energy sources such as the industrial sector, transport, nuclear, and others.

Among these sources are gas-turbine power plants, which waste exhaust heat into the atmosphere.

In this work, combined cycle power plant configurations are studied.

The first cycle engine uses a simple Brayton cycle as the topping cycle and a supercritical carbon dioxide power cycle as the bottoming cycle. The topping cycle is expected to use methane (natural gas, CH_4) as its fuel. Waste heat from the topping cycle is used to power the bottoming cycles.

The station named the Hilla Gas Station located in the Babil governorate in the middle of Iraq was chosen due to the need of the city to increase the production capacity of

electric energy and due to the fact that it consists of four units each unit produces 26.83 megawatts and the target capacity to reach it after the addition of supercritical carbon dioxide gas stations is 35 megawatts, this means raising energy production to about 40% of the unit's production capacity without addition.

And this increase does not consume additional fuel, but rather a recovery of wasted energy from the exhaust, and these stations do not take up large areas and cost less than other types of stations.

3.1. PROPOSED WASTE HEAT RECOVERY SYSTEM

In the current work, we have designed a process to restore lost heat to the atmosphere and to use it in the production of electric power in order to find a practical solution to take advantage of the lost heat in all fields and achieve green development. The design of the power plant, where CO_2 gas is the liquid of its work, is based on previous studies conducted by Zhiyuan Liu [19] and Gotelip [47], the composite chart of the cycle contains two main parts, as illustrated in figure 3.1.

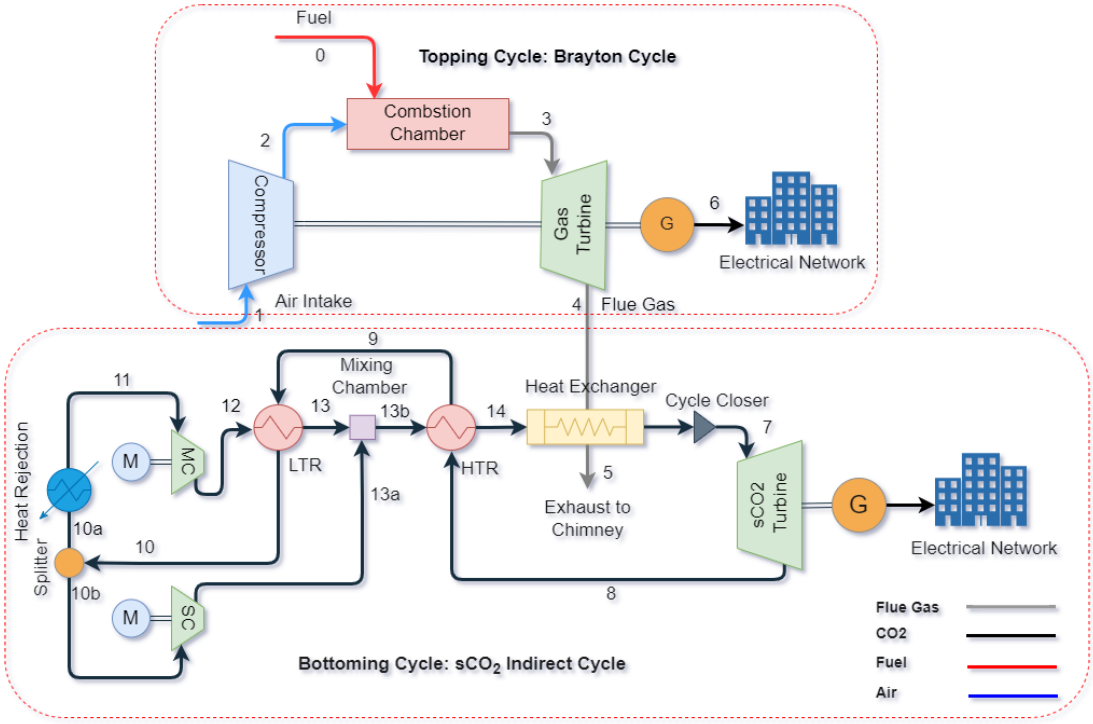

Figure 3.1. Combined cycle power plant, Topping Cycle: Gas Brayton Cycle, Bottoming Cycle: sCO_2 Indirect Cycle.

In order to establish the interface between the parts of the system described in the above outline, we will write all the connections between the station components through the following table:

Table 3.1. Summary of State Points.

State point		Component outlet	Component inlet
Topping Cycle	0	Fuel Storage	Combustion Chamber
	1	Air Intake	Compressor
	2	Compressor	Combustion Chamber
	3	Combustion Chamber	Gas Turbine
	4	Gas Turbine	Heat Exchanger
	5	Heat Exchanger	Chimney
Bottoming Cycle	6	Heat Exchanger	Cycle Closer
	7	Cycle Closer	CO_2 Turbine
	8	Co2 Turbine	HTR
	9	HTR	LTR
	10	LTR	Splitter
	10a	Splitter	HRU
	10b	Splitter	SC
	11	HRU	MC
	12	MC	LTR
	13	LTR	Merge
	13a	SC	Merge
	13b	Merge	HTR
	14	HTR	Heat Exchanger

3.1.1. Topping cycle: Gas Brayton Cycle

This station that has name "Hilla gas station" was established in 2012 with 3 units, each unit has a capacity of 10 megawatts and in 2016, 4 additional units were added by GE Oil&Gas, each unit has a capacity of 26.83 megawatts, which will be developed in this study, the course parameters were obtained by the station officials as shown in the following table:

Table 3.2. Parameters of Topping cycle.

NO	Parameters	Value
1	Station Name	Hilla Gas Station
2	Type of Cycle	Brayton Cycle
3	Station Capacity (MW)	26.83
4	Heat rate(Kj/KWh)	12687
5	Type of Fuel	Natural Gas (CH_4)
6	Exhaust Temperature avg. (°C)	488-515
7	Mass flow (Kg/s)	126.8
8	Air inlet temperature(°C)	13-38
9	Pressure ratio	10.5:1
10	Model of Turbine and Generator	MS5001PA

The output values of the power plants vary over the course of the year, depending on the value of the loads on the grid and sometimes reach the fire. The following chart shows the electricity produced at the rate of each month and the temperatures of the exhaust gas and mass:

Table 3.3. Topping Cycle Outlet.

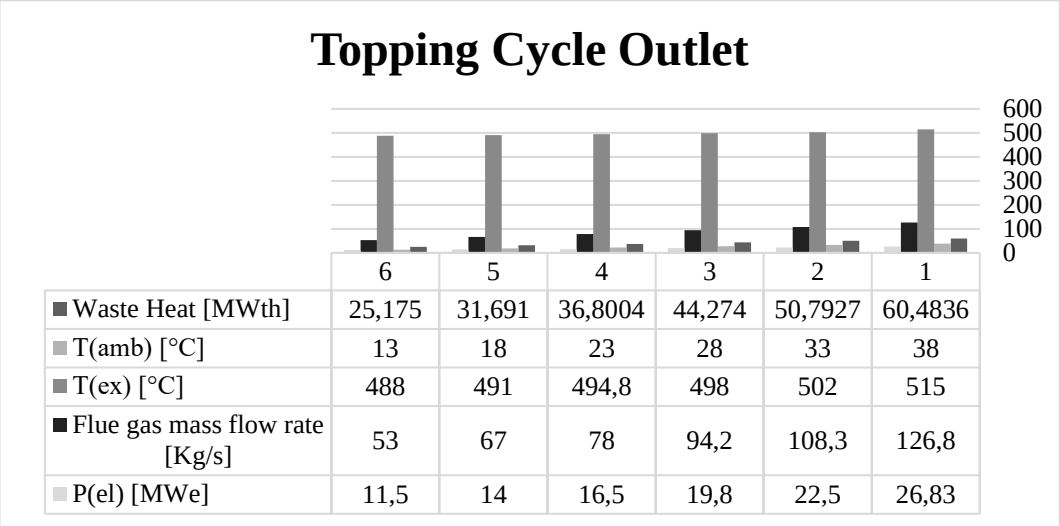

	6	5	4	3	2	1
Waste Heat [MWth]	25,175	31,691	36,8004	44,274	50,7927	60,4836
T(amb) [°C]	13	18	23	28	33	38
T(ex) [°C]	488	491	494,8	498	502	515
Flue gas mass flow rate [Kg/s]	53	67	78	94,2	108,3	126,8
P(el) [MWe]	11,5	14	16,5	19,8	22,5	26,83

3.1.2. Bottoming Cycle Supercritical Carbon Dioxide Cycle

In the RRC configuration, a portion of the low-pressure working fluid is directed to the Heat Rejection Unit (HRU) at (point 10a). As shown in (point 11), the fluid has now reached the cycle's lowest temperature. It is then compressed by the main compressor at (point 12) and subsequently heated at (point 13) through the Low Temperature Recuperator (LTR). The fraction that remains (point 10b) is divided immediately before the HRU and is then compressed to the maximum pressure of

the cycle (point 13a) by a secondary compressor. The two streams are ultimately combined at the entrance of the HTR's cold side, namely at (point 13b). Recompression improves the efficiency of the cycle by equalizing the heat capacity of the hot and cold streams in the LTR, thereby reducing temperature differences in the heat exchanger and minimizing irreversibility associated with heat transfer. The working fluid is preheated in the High Temperature Recuperator (HTR) to complete the process (point 14). The HTR cools down the hot CO_2 that comes out of the turbine (point 8). The temperature differences are minimized at the cold end of the HTR and tend to increase towards the hot end. This is because high-pressure fluid always has a slightly higher specific heat than a low-pressure stream. Consequently, the efficiency of the thermodynamic cycle is enhanced, but the internal recuperative process's high effectiveness may restrict the utilization of the variable temperature heat source, thus restricting the thermal power input and power output of the cycle.

Table 3.2. Heat source data and cycle design assumptions.

Parameter	**Value**
Heat source mass flow rate $\dot{m}_{hs}$, kg/s	125.2
Heat source temperature $T_{hs,max}$, °C	510
Minimum heat source temperature $T_{hs,min}$, °C	340
Heat source specific heat Cp_{hs}, kJ/kgK	1.063
Maximum admissible cycle temperature, °C	550
Maximum admissible cycle pressure, bar	250
Minimum cycle temperature, °C	35
LTR pinch point ΔT_{LTR},°C	10
HTR pinch point ΔT_{HTR},°C	10
HX pinch point ΔT_{HX},°C	25
PHE CO2 $\Delta p, bar$	2
HRU CO2 ($\Delta p/pin$)	0.5%
Recuperators hot side ($\Delta p/pin$)	0.5%
Recuperators cold side ($\Delta p/pin$)	0.5%
Turbine isentropic efficiency, $\eta_{turbine}$	0.9
Main compressor efficiency, η_{MC}	0.85
Secondary compressor efficiency η_{SC}	0.85
Generator/motor efficiency $\eta_{me,t}$ / $\eta_{me,c}$	0.96

3.2. THERMODYNAMIC MODEL

Energy and Exergy Analysis and Economic Analysis of the plant has been performed with the use of the thermo-dynamic and thermos-economic tools. The thermodynamic

model is done using Python –TESPy[49]. Thermo-physical properties of flue gas were taken from a plant.

First, we calculate the amount of wasted heat from the upper station that will be recovered in the lower station through the heat capacity law (Equation (3.1)).

$$\dot{Q} = \dot{m}\, cp\, (To - Ti) \tag{3.1}$$

Where:

$\dot{Q}$: Amount of heat energy transferred (Watt)
$\dot{m}$: exhaust mass flow rate (Kg/s)
cp: heat capacity of flue gases($kj/kg.$℃)
To: Exhaust temperate (°C)
Ti: input air temperature (°C)

The general energy balance of a thermodynamic open system in steady-state (Equation (3.2)), the choice of parameters to describe the state of the fluid falls to enthalpy and pressure.

$$\dot{Q} - \dot{W} = \sum m_{out} \cdot h_{out} - \sum m_{in} \cdot h_{in} \tag{3.2}$$

$$\sum \dot{m}_{in} = \sum \dot{m}_{out} \tag{3.3}$$

$\dot{Q}$ And $\dot{W}$ refer to the heat and the workflow, respectively. The main indexes used to evaluate the system performance are the cycle net efficiency (including HRU auxiliaries consumption η_{cycle}, the heat recovery factor χ and the overall recovery efficiency η_{rec} defined as [40]:

$$\eta_{cycle} = \frac{\dot{W}_{net}}{\dot{Q}_{in}} = \frac{\dot{W}_{turb} - \dot{W}_{mc} - \dot{W}_{sc} - \dot{W}_{HRU}}{\dot{Q}_{in}} \tag{3.4}$$

$$\chi = \frac{\dot{Q}_{in,cycle}}{\dot{Q}_{hs,max}} = 1 - \frac{T_{stack} - T_{hs,min}}{T_{hs,max} - T_{hs,min}} \tag{3.5}$$

$$\eta_{rec} = \chi \cdot \eta_{cycle} = \frac{\dot{W}_{net}}{\dot{Q}_{hs,max}} \quad (3.6)$$

3.2.1. Thermodynamic Relations for Components of Power Cycle

In this section, we determine the thermal equations for the main station parts, their respective exergy balance equations, as well as other components available in the software.

A turbine is regarded as an adiabatic component. Hence, the power transmitted $\dot{W}$ may be determined by multiplying the mass flow rate $\dot{m}$ with the difference in enthalpy h between the component's input (index in) and output (index out)[50].

$$\dot{W} = \dot{m} \cdot (h_{out} - h_{in}) \quad (3.7)$$

The isentropic efficiency is a crucial parameter for adiabatic turbines. It quantifies the ratio between the actual change in enthalpy and the greatest possible change in enthalpy during an isentropic operation, given a certain pressure change.

$$\eta_{turb} = \frac{(h_{in} - h_{out})}{(h_{in} - h_{out,s})} \quad (3.8)$$

The enthalpy at the outlet of the isentropic process, denoted as $h_{out,s}$, is determined by using Equation (3.9) with the outlet pressure and input entropy of the process.

$$h_{out,s} = h(p_{out,}s\ (p_{in}, h_{in})) \quad (3.9)$$

The same principle that has been applied to turbines will apply to compressions, but in reverse, because of compressors is the process that occurs within the compressors, so the method of calculating efficiency will be as in an equation. (3.10)

$$\eta_{s,c} = \frac{(h_{out,s} - h_{in})}{(h_{out} - h_{in})} \quad (3.10)$$

Only heat is transferred via heat exchangers. We overlook heat losses to the surrounding air. Equation (3.3) states that the fluid on a heat exchanger's cold side (index 2) receives all of the heat produced by the heat exchanger's hot side (index 1). Equation (3.4), which is used to determine the heat transferred $\dot{Q}$.

$$\dot{Q} = \dot{m} \,.\, (h_{out1} - h_{in1}) \tag{3.11}$$

$$\dot{m}_{in1}.\,(h_{out1} - h_{in1}) = \dot{m}_{in2}.\,(h_{out2} - h_{in2}) \tag{3.12}$$

In some cycles, there are branches and each branch of a particular path, and then these branches meet in a single pallet called the Merge point, and the number of these branches is coded i, assuming that there will be no loss of heat or energy to the ocean, as in an equation (3.13).

$$\sum_i \dot{m}_{in,i}.\,h_{in,i} = \dot{m}_{out}.\,h_{out} \tag{3.13}$$

After we get the energy produced in the turbine $\dot{W}$ as in the equation (3.7), which will go through the shaft to the generator, and assuming the generator's efficiency is $\eta_{el,gen}$, the power output of the generator $\dot{W}_{el,gen}$ is calculated by the equation (3.14), taking into account the mechanical and electrical losses.

$$\dot{W}_{el,gen} = \dot{W} * \eta_{el,gen} \tag{3.14}$$

In the motors, it consumes electricity to rotate the pumps or compressors or fans, the electrical energy consumption $\dot{W}_{el,mot}$ can be calculated by dividing the pump or compressor or fan energy $\dot{W}$ into the motor efficiency $\eta_{el,mot}$ as in equation (3.15).

$$\dot{W}_{el,mot} = \frac{\dot{W}}{\eta_{el,mot}} \tag{3.15}$$

3.3. EXERGY ANALYSIS

Exergy (Ex) is defined as the amount of work (=entropy-free energy) a system can perform when it is brought into thermodynamic equilibrium with its environment[51], The total exergy rate is the product of mass flow rate and specific exergy, which consists of the sum of physical e^{PH}, chemical e^{CH}, kinetic energy e^{KN}, and potential exergy e^{PT}. Effects associated with nuclear, magnetic, or electric processes are not considered[52].

$$\dot{E} = \dot{m}(e^{PH}+e^{CH}+e^{KN}+e^{PT}) \tag{3.16}$$

In the calculations that entered into the exergy analysis, we're going to do a physical exergy e^{PH} first, as in an equation (3.17), which will enter into each of the following thermodynamic parameters for state (p, T, h, s), thermodynamic parameters of the restricted reference state 0 ($p0, T0, h0, s0$). Then, it is feasible to divide physical exergy into thermal e^{T} and mechanical e^{M} components using Equations (3.18) and (3.19). The first phase involves isobarically adjusting the temperature of the fluid to match the surrounding temperature in order to acquire the thermal exergy. The second stage involves obtaining the mechanical exergy by isothermally adjusting the fluid's pressure to the ambient level[53].

$$e^{PH} = (h - h0) - T0(s - s0) = e^{T} + e^{M} \tag{3.17}$$

$$e^{T} = \big(h - h(p,T0)\big) - T0(s - s(p,T0)) \tag{3.18}$$

$$e^{M} = \big(h(p,T0) - h(p0,T0)\big) - T0.(s(p,T0) - s(p0,T0)) \tag{3.19}$$

The concept of exergy destruction measures the extent of thermodynamic inefficiencies that are linked to a particular operation. These phenomena may arise via chemical reactions, heat transmission, mixing, and friction, and are present in all practical systems. This technique may be used to identify the components that experience the most significant exergy degradation and the mechanisms responsible

for it. Considering that the process operates at steady-state conditions, the exergy balance for component k is used to calculate its exergy destruction $\dot{E}_{D,k}$. The balance contains different terms for exergy transport by heat transfer $\dot{E}_{q,j,k}$ and power $\dot{W}_k$ as well as with transport of matter at the inlet $\dot{E}_{i,k}$ and exit $\dot{E}_{e,k}$ of component k [54].

$$\dot{E}_{D,k} = \sum_j \dot{E}_{q,j,k} + \dot{W}_k + \sum_i \dot{E}_{i,k} - \sum_e \dot{E}_{e,k} \tag{3.20}$$

The exergy efficiency of a component k is given as:

$$\varepsilon_k = \frac{\dot{E}_{P,k}}{\dot{E}_{F,k}} \tag{3.21}$$

The exergy rates $\dot{E}_{P,k}$ and $\dot{E}_{F,k}$ represent the exergy rates of the product and fuel, respectively, for the component k being evaluated. The overall system exergy efficiency is defined as:

$$\varepsilon_{tot} = \frac{\dot{E}_{P,tot}}{\dot{E}_{F,tot}} = 1 - \frac{\dot{E}_{D,tot} + \dot{E}_{L,tot}}{\dot{E}_{F,tot}} \tag{3.22}$$

Parameters $\dot{E}_{P,tot}$ and $\dot{E}_{F,tot}$ represent the exergy rates of the product and fuel in the entire system.The system's actual thermodynamic inefficiencies may be established by computing the total of the component exergy destruction $\dot{E}_{D,tot}$ as well as the exergy losses from the overall system $\dot{E}_{L,tot}$. The exergy destruction ratios $y_{D,k}$ for a component may be computed based on the information obtained from the whole system as in equation (3.23)[54].

$$y_{D,k} = \frac{\dot{E}_{D,k}}{\dot{E}_{F,tot}} \tag{3.23}$$

3.4. THERMO-ECONOMIC MODEL

Aside from power generating efficiency, the investment cost of a power generation system is also a crucial factor to be taken into account when considering

commercialization. Table (3.4) displays the cost functions of the main components in a supercritical CO_2 Brayton cycle. The cost functions of the compressor, turbine, and generator are fitted using a power function based on data from the year 2003. The chemical economic plant cost index (CEPCI) is used to account for the impact of inflation[19]. The overall cost function of the whole thermal system may be expressed as:

$$C_{TPC} = \frac{CEPCI_{2023}}{CEPCI_{2003}} . \left(C_{2003}^{comp} + C_{2003}^{reac} + C_{2003}^{turb} + C_{2003}^{HX} + C_{2003}^{cond}\right) \quad (3.24)$$

Where C is meaning cost ($) of each component and which can calculate the cost of each one by equations in table (3.3)[55]. The abbreviation "CEPCI2023" refers to the Chemical Engineering Plant Cost Index for the year 2023 Aug = (798.7).

Table 3.3. Approximate Cost Scaling of each component.

Component	**Approximate Cost Scaling**
Compressors ($)	$643.15(W\ [kW])^{0.9142}$
Recuperator ($)	$5.2(UA(W/K))^{0.8933}$
Turbines ($)	$9923.7(W\ [kW])^{0.5886}$
Primary Heat Exchanger ($)	$17.5(UA(W/K))^{0.8778}$
Air Coolers / Condensers ($)	$76.25(UA(W/K))^{0.8919}$

Other costs are calculated as a proportion of the total cost of that plant, which includes operating and maintenance costs as in equation (3.25).

$$C_{O,M} = C_{fuel} + C_{ins} + C_{lab} + C_{main} \quad (3.25)$$

which specifically include the cost of fuel, guarantee, employment and maintenance and are calculated in accordance with the equivalents in the table(3.4)[19].

Table 3.4. Approximate Cost Scaling of operating and maintenance.

Component	**Approximate Cost Scaling**
Fuel $\boldsymbol{C_{fuel}}$, $	$C_{PQ} * \dot{Q}_{th}$
Insurance $\boldsymbol{C_{ins}}$, $	$0.01 * C_{TPC}$
Labor $\boldsymbol{C_{lab}}$, $	$0.02 * C_{TPC}$
Maintenance $\boldsymbol{C_{main}}$, $	$0.015 * C_{TPC}$

The levelized cost of electricity (LCOE) is calculated from equation (3.26)[56]:

$$LCOE = \left({C_{TPC} * CRF + C_{O,M}} \Big/ {W_{net} * \ t_y} \right) \tag{3.26}$$

Where the load operation hours t_y is 8000 $h/year$ and the CRF represents capital recovery cost it given as:

$$CRF = {i * (1 - i)^n} \Big/ {((1 - i)^n - 1)} \tag{3.27}$$

Where the economic life time n = 20 years, and the interest rate $i \ = \ 6\%$.

3.5. ENVIRONMENTAL ANALYSIS

Waste heat appears during almost every step of energy conversion and is rejected by the environment in many cases. In order to raise process efficiencies, solutions for further use have to be found [7]. Taking advantage of thermal energy wasted in the atmosphere and the emissions of double-carbon gases is a direct challenge due to their direct effect on global warming and atmospheric warming. In our study, we will extract the heat of the exhaust from it for the generation of electricity that will feed the electricity system. By increasing the use of waste heat in low-, medium-, and high-temperature sources, there will be greater energy production and less gas emissions. To determine the environmental impact of this study and since it obtains energy from a waste source of heat, we will calculate the equivalent of that energy from methane as in an equation of (3.28).

$$C_C = 32.15 - (0.234 \times H_V)$$

Where C_C represents factor of carbon emissions in t C/TJ and H_V represents gross calorific value of Natural gas liquid, with a calorific value is 42.83 TJ/kiloton [57].

3.6. SIMULATION OF THERMAL CONVERSION PROCESSES BY USING TESPY

TESPy is an acronym for "Thermal Engineering Systems in Python" that was created by MIT Institute [49] and offers a robust simulation toolbox for thermal engineering facilities, including power plants, district heating systems, and heat pumps. The module is an external extension of the Open Energy Modelling Framework (OEMOF) and may be used independently as a package. The most important feature of the Tespy instrument is the following points:

- Ability to calculate stationary operation to design the process of your plant.
- Predictability of the off-design behavior of your plant using underlying characteristics for each of the plant components.
- It has most of the simple and complex station components, such as turbines, pumps, compressors, heat exchangers, pipes, mixers, and splitters as well as some advanced components (derivatives of heat exchangers, drum).
- Provides physical properties of fluids CoolProp such as water, ammonia, carbon dioxide, etc.

To carry out the design and energy and exergy analysis process, we first need to identify the environmental requirements surrounding the station, temperature, and pressure, input the parameters of the cycle and strand them as in the proposed course outline, and then define the parameters for each element of the cycle and as required by the system, such as input the mechanical efficiency of the turbines and compressors, and then introduce the thermal value that enters that plant through the heat recovery system, requesting that the results be printed in a meaningful manner, encoded by the specified variables, and calculating the power and efficiency of the station. This tool will calculate the design of each part of the station, such as the mass of the working fluid, the heat rejected from the coolant, the temperature, the pressure, the enthalpy and the entropy of each point, as well as the calculation of the exergy distribution for each of its components.

PART 4

RESULTS AND DISCUSSIONS

In this chapter, the results of the thermal analysis, exergy analysis, economic and environmental analysis and various operational requirements will be reviewed. In general, the cycle system consists of a top cycle (Gas power plant), which is a friendly unit for a 26.83 MW_e design power plant, this power plant is linked to the bottom cycle (sCO_2 power plant) through heat exchangers that transfer heat to the bottom cycle operating fluid (CO_2), only by relying on the recovered heat source is the sCO_2 power plant operated and power generation for the electrical system. Through Table (4.1), we're going to check the validation of the model built by Python and through the TESpy tool.

Table 4.1. Validation of the Gas Brayton cycle model.

Parameters	Unit	Real values	Present Model
P_{amb}	bar	1.013	1.013
T_{amb}	°C	36	36
Pressure ratio	-	10.5:1	10.5:1
Exhaust Flow	Kg/s	nan	104.5
Fuel consumption	Kg/s	1.69	1.68
Exhaust Temperature	°C	511	510.9
Power output	MW	22	22
Thermal efficiency	%	nan	26.18

4.1. THERMODYNAMIC ANALYSIS

In this section, six operational cases were approved for the upper station by electrical power requirements in 2022 in Iraq. The thermodynamic analysis was obtained according to the gas mass flow rate from the variable upper station from 53 to 126.8 (Kg/s), and the temperature from 488 to 515 (°C). These changes are due to the change in generating capacity and the temperature of entry according to the schedule of temperature and variable 15 to 38 (°C) as shown in Table (4.2).

Table 4.2. Properties of flue gas.

State	Month	GT Power (MW)	Flue gas mass flow rate (Kg/s)	T_{ex} (°C)	T_{amb}(°C)	Waste Heat (MW)
1	July	26.83	126.8	515	38	60.4836
2	May	22.5	108.3	502	33	50.7927
3	March	19.8	94.2	498	28	44.274
4	January	16.5	78	494.8	23	36.8004
5	November	14	67	491	18	31.691
6	December	11.5	53	488	13	25.175

In table 4.3, all the physical properties of the combined cycle points were calculated, and a T-S diagram of the CO_2 cycle was drawn according to the output properties that we got as shown in figure (4.1). And so all the energy duties are calculated in the table (4.4).

Table 4.3. Properties for each state for the combined cycle at the full load condition.

State	m (kg/s)	Pressure (bar)	Temperature (°C)	Enthalpy (kJ/kg)	Entropy (kJ/kg. K)
0	2.1	11.64	38	929	5.43
1	124.7	1.013	38	311.7	6.7037
2	126.8	10.64	329.6	610.4	6.8775
3	126.8	10.64	940	1426	7.5856
4	126.8	1.013	516	920.8	6.864
5	126.8	1.013	380.8	472	6.3437
6	334.5	250	510	988	2.6388
7	334.5	250	510	988	2.6388
8	334.5	77.95	380.7	845.4	2.6632
9	334.5	76.94	331.5	789.2	2.5763
10	334.5	75.15	179.8	618.5	2.2563
10a	273	75.15	179.8	618.5	2.2563
10b	61.5	75.15	179.8	618.5	2.2563
11	273	75	59.8	465	1.8586
12	273	258.4	174.8	541.8	1.8586
13	273	257.5	326.5	751	2.2894
13a	61.5	257.5	326.5	751	2.2894
13b	334.5	275.5	326.5	751	2.2894
14	334.5	257	370.9	807.2	2.3803

Table 4.4. Energy duties of the co2 power plant.

Parameters	**Unit**	**Value**
Heat input	KW	59780
Turbine power	KW	47710
Main Compressor power	KW	-20980
Sec. Compressor power	KW	-8154
Electrical output power	KW	16113
Cooler (HRU) Power	KW	-605.4

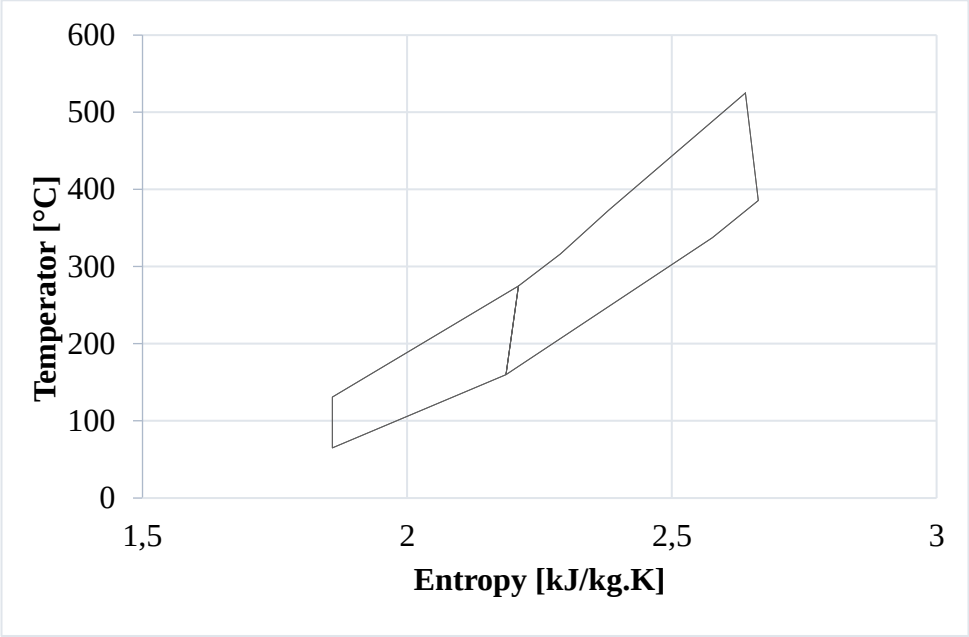

Figure 4.1. T-S diagram of CO_2 cycle.

Figure (4.2) shows the value of electricity production, efficiency, and comparison of the value of the production of the upper station during the cases considered during the year, and shows here that the lower the temperature of the ocean, the greater the production and the greater the efficiency.

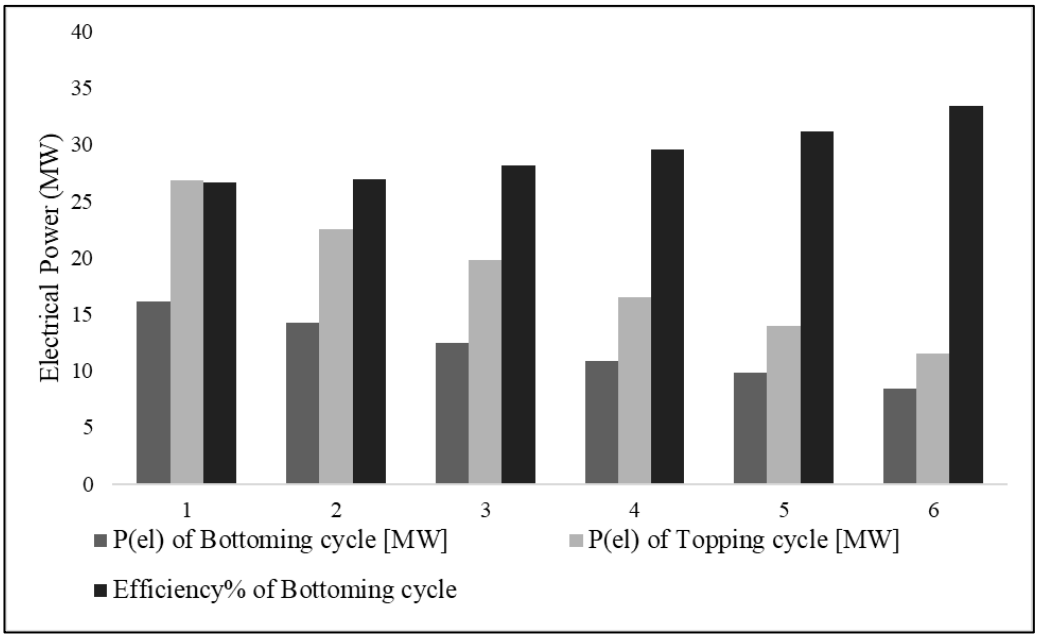

Figure 4.2. Value of production and efficiency of the cycles.

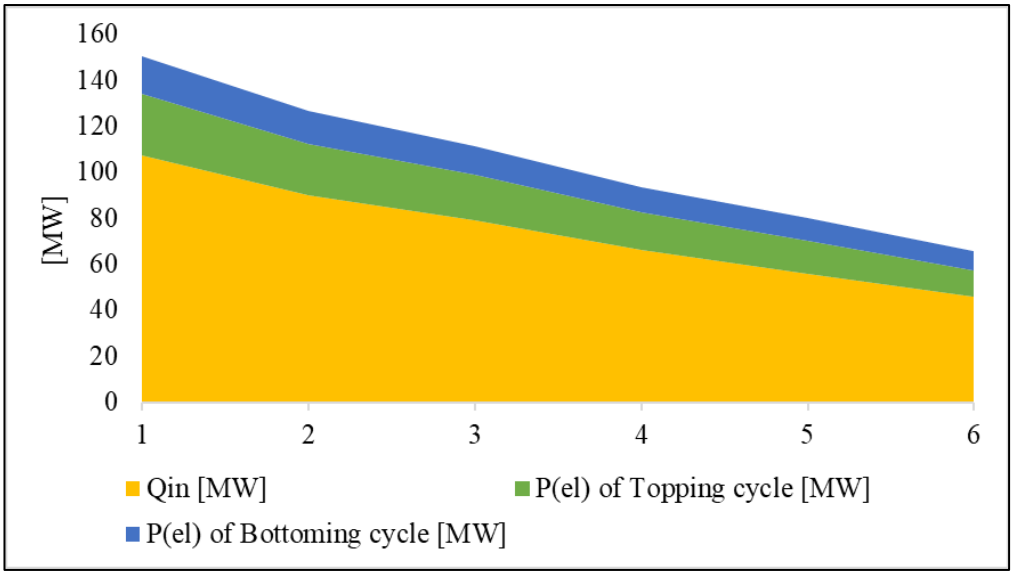

Figure 4.3. Comparison of thermal energy input and the amount of energy generated per cycle.

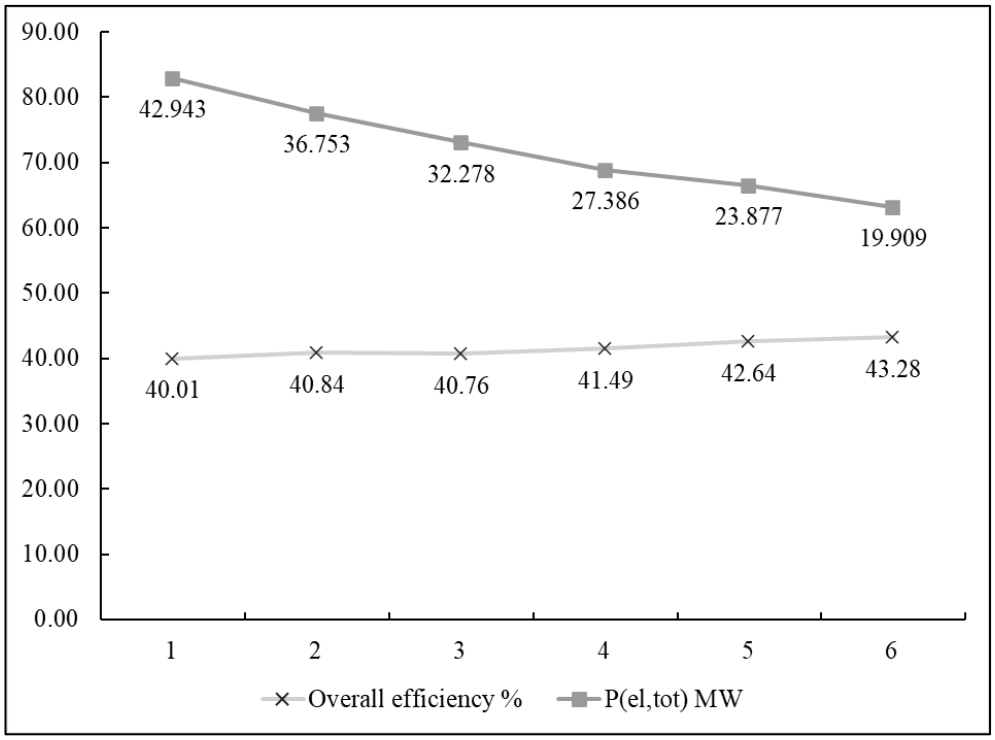

Figure 4.4. Total power output and overall efficiency chart.

Table 4.5. Comparisons of different testing facilities of sCO_2 power plant.

Institution	**Cycle layout**	**Net power (KW)**	**Turbomachi-nery**	**Heat source**	**Heat source capacity (KW)**
Our Study	Recompressed Recuperative Cycle	16113	2 recuperator 2 compressor 1 turbine	Flue gas	59780
Echogen [58]	Pre-heating /split expansion	8000	1 compressor 2 turbines	Flue gas	33000
SwRI, GE, Thar, Aramco, EPRI [59]	Simple recuperated cycle	1000	1 recuperator 1 compressor 1 axial turbine	Flue gas	N/A
SNL [60]	Recompression	300	2 TAC	Electric	780
KAPL [24]	Simple regenerated	100	1 TAC 1 turbines	Electric	835
KAIST/KAERI [61]	Simple regenerated	300	1 TAC 1 turbine 1 compressor	Electric	1300
KIER [62]	Simple regenerated	80	2 turbine 1 compressor	Flue gas	611

4.2. EXERGY ANALYSIS

The results of the extraction analysis attached to the table, which is dependent on pressure and ocean temperature and which has been taken in several cases, are shown in the table in the nose and the net power generation of the process is linked to the product, the practice rate for the process associated with the temperature is, the overall performance efficiency, is 47.6 percent, and the remaining operational situations will be explained in the figure(4.3)

Table 4.6. Exergy analysis results of the sCO2 power cycle, overall process.

$\dot{E}_{F.total}$(MW)	$\dot{E}_{P.total}$(MW)	$\dot{E}_{D.total}$(MW)	ε_{tot}(%)
33.81	16.11	17.7	47.6

Table 4.7. Exergy analysis results of the sCO2 power cycle, components.

Component k	$\dot{E}_{F.k}$(MW)	$\dot{E}_{P,k}$(MW)	$\dot{E}_{D,k}$(MW)	ε_k(%)	$y_{D,k}$(%)
Turbine	50.26	46.6	3.499	93.04	10.35
Main Compressor	22.07	18.77	3.294	85.08	9.741
Sec. Compressor	8.578	7.511	1.067	87.56	3.155
Heat Exchanger	33.81	33.55	0.2629	99.22	1.195
HTR	23.74	22.73	1.01	95.75	2.985
LTR	9.761	9.357	0.404	95.86	1.195
Water Cooler	8.164	nan	8.164	nan	24.14

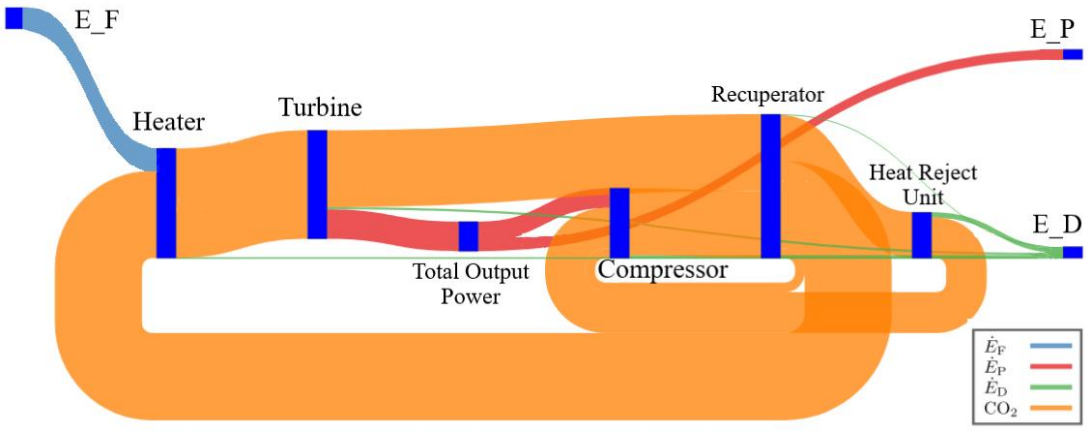

Figure 4.5. Sankey diagram of functional groups of sCO_2 power cycle for work flow.

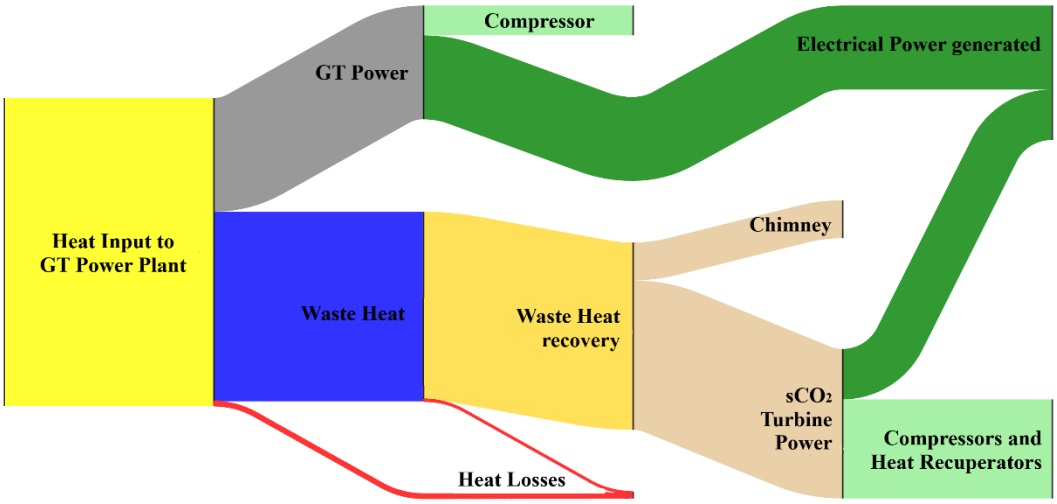

Figure 4.6. Sankey diagram of functional groups of sCO_2 power cycle for energy.

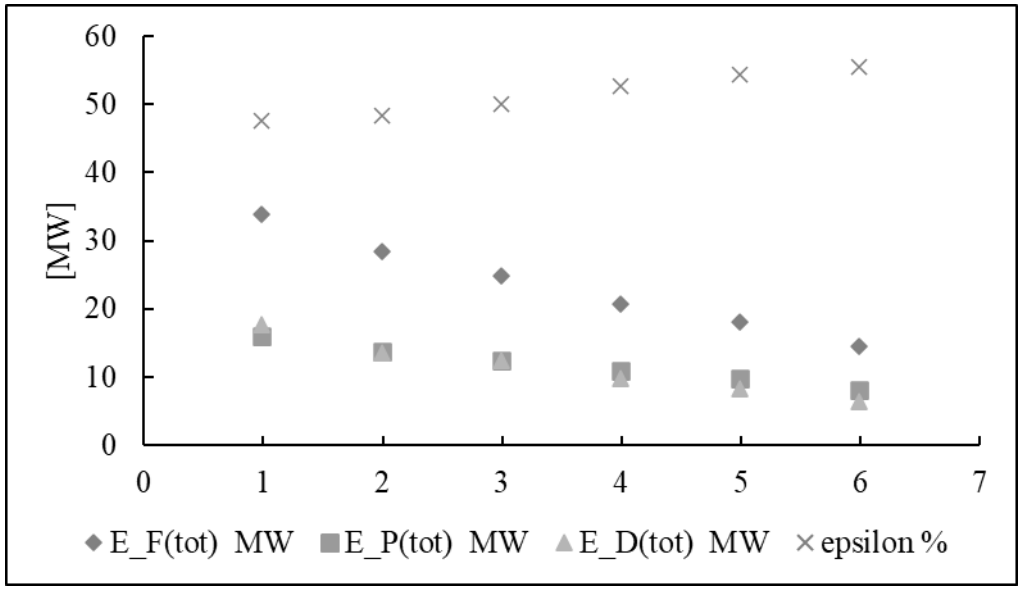

Figure 4.7. $\dot{E}_{P,tot}$, $\dot{E}_{F,tot}$, $\dot{E}_{D,tot}$, and ε_{tot} at different operating states.

4.3. THERMOECONOMIC MODEL

Thermo-economic analysis is very important when proposing and studying any design or addition because of course it's a key indicator of whether this design is economically useful and over the years of operation, in this section we will review the total cost of the plant C_{tpc} and the cost of electricity per KWh LCOE according to the six design lines. And considering the life time of the station is 20 years.

Table 4.8. Economic analysis results at 6 six design lines.

State	Item	unit	value
1	LCOE	$/kWh	0.01625
	C_{tpc}	$/h	639
2	LCOE	$/kWh	0.01615
	C_{tpc}	$/h	562
3	LCOE	$/kWh	0.01601
	C_{tpc}	$/h	497
4	LCOE	$/kWh	0.01576
	C_{tpc}	$/h	420
5	LCOE	$/kWh	0.01518
	C_{tpc}	$/h	367
6	LCOE	$/kWh	0.01450
	C_{tpc}	$/h	298

4.4. ENVIRONMENTAL ANALYSIS

In calculating the amount of carbon resulting from the burning of liquid methane needed by the sCO_2 station to generate 16.11 MW of electricity, as shown in table 4.7, the resulting amount was found to be 4.82 ton per hour.

Table 4.9. Emission reduction by heat recovery

Parameters	Unit	Value
Cc	tC/TJ	22.127
Energy needed	TJ/h	0.2178
Emission reduction	ton/h	4.82

The amount of the reduced emissions was explained by the heat recovery process in the six design cases as in the figure of (4.7).

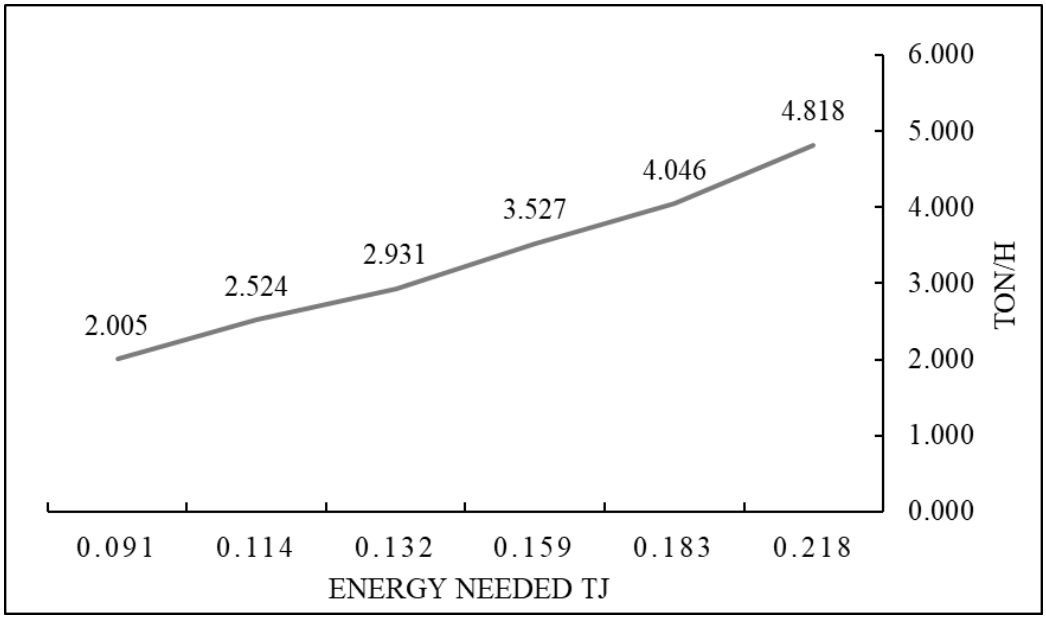

Figure 4.8. Reduction of emissions in each operational point.

PART 5

CONCLUSIONS

The performance of the supercritical carbon dioxide cycle on a waste source of heat, which represents the first Hilla gas station, has been studied and evaluated during different periods of the year. This study aims at developing future solutions for power supply and reducing air pollution. The design calculations were done through the TESpy tool, and the corresponding working environment was set up in Python, in this study, energy analysis, exergy analysis, thermo-economic analysis, and environmental impact of the proposed plant were conducted. The main findings can be summarized in the following points:

- The waste heat energy that can be recovered varies from 60.4 to 25.17 MW Thermal by variable operating points.
- The electrical energy produced during the various case periods, at full load, the greatest generation of electricity by the Brayton cycle was 26.83 MW and 16.113 MW for the sCO_2 cycle. At the lowest load, it was 11.5 MW by the Brayton cycle and 8.4 MW by the sCO_2 cycle.
- The highest thermal efficiency obtained for the sCO_2 cycle was at the lowest load of 33.4%, and 26.64% at full load.
- The total efficiency of the combined cycle has been improved to 40.01% at the lowest level and 43.28% at the highest level.
- The total fuel exergy for all components of the sCO_2 cycle was 33.1 MW, of which 16.11 MW was used as product exergy and the remaining 17.7 MW was distributed out of the system, and the exergy efficiency was 47.6%. On the other side, at the lowest operating point, the was 14.56 MW and was 8.085 MW while what was destroyed outside was 6.474 MW and was 55.53%.
- In the area of economic analysis, the highest cost per kilowatt hour was 0.01625$ and the cost of setting up the additional sCO_2 cycle power station

was $639 per operational hour, which was assumed to work 8,000 hours per year.

- The lowest of emissions this station can reduce is 2 tons/hour, up to 4.5 tons/hour at fuel points.

With regard to the determinants, the sCO_2 cycle at the medium operating temperatures of 450 - 550 after cooling CO_2 by HRU, the pressure and temperature should be higher than the pinch point of the CO_2 gas, in which carbon dioxide becomes a gas state again.

After this study, it is possible in future studies to design another type of supercritical carbon dioxide cycle on the same operational requirements and to make a systematic comparison between the results obtained from the cycles and select best the options according to the results of the comparison.

REFERENCES

[1] NOAA, “Global carbon dioxide growth in 2018 reached 4th highest on record.” [Online]. Available: https://www.noaa.gov/news/global-carbon-dioxide-growth-in-2018-reached-4th-highest-on-record

[2] IEA, “Global CO2 Emissions in 2019 – Analysis.” [Online]. Available: https://www.iea.org/articles/global-co2-emissions-in-2019

[3] BP Statistical Review of World Energy, “Global primary energy consumption by source.” [Online]. Available: https://ourworldindata.org/grapher/global-energy-substitution

[4] Z. Y. Xu, R. Z. Wang, and C. Yang, “Perspectives for low-temperature waste heat recovery,” *Energy*, vol. 176, pp. 1037–1043, Jun. 2019, doi: 10.1016/j.energy.2019.04.001.

[5] Z. J. Yong, M. J. K. Bashir, C. A. Ng, S. Sethupathi, J. W. Lim, and P. L. Show, “Sustainable waste-to-energy development in Malaysia: Appraisal of environmental, financial, and public issues related with energy recovery from municipal solid waste,” *Processes*, vol. 7, no. 10. MDPI AG, 2019. doi: 10.3390/pr7100676.

[6] N. Galanis, E. Cayer, P. Roy, E. S. Denis, and M. Désilets, “Electricity generation from low temperature sources,” *J. Appl. Fluid Mech.*, vol. 2, no. 2, pp. 55–67, 2009, doi: 10.36884/jafm.2.02.11870.

[7] C. Forman, I. K. Muritala, R. Pardemann, and B. Meyer, “Estimating the global waste heat potential,” *Renewable and Sustainable Energy Reviews*, vol. 57. Elsevier Ltd, pp. 1568–1579, May 01, 2016. doi: 10.1016/j.rser.2015.12.192.

[8] F. Sun, J. Li, L. Fu, Y. Li, R. Wang, and S. Zhang, “New configurations of district heating and cooling system based on absorption and compression chillers driven by waste heat of flue gas from coke ovens,” *Energy*, vol. 193, p. 116707, 2020, doi: 10.1016/j.energy.2019.116707.

[9] G. Liao, J. E, F. Zhang, J. Chen, and E. Leng, “Advanced exergy analysis for Organic Rankine Cycle-based layout to recover waste heat of flue gas,” *Appl. Energy*, vol. 266, no. January, p. 114891, 2020, doi: 10.1016/j.apenergy.2020.114891.

[10] Y. Dou *et al.*, “Innovative planning and evaluation system for district heating using waste heat considering spatial configuration: A case in Fukushima, Japan,” *Resour. Conserv. Recycl.*, vol. 128, pp. 406–416, 2018, doi: 10.1016/j.resconrec.2016.03.006.

[11] C. Li and H. Wang, “Power cycles for waste heat recovery from medium to high temperature flue gas sources – from a view of thermodynamic optimization,” *Appl. Energy*, vol. 180, pp. 707–721, 2016, doi: 10.1016/j.apenergy.2016.08.007.

[12] L. Liu, Q. Yang, and G. Cui, “Supercritical carbon dioxide(S-co2) power cycle for waste heat recovery: A review from thermodynamic perspective,” *Processes*, vol. 8, no. 11. MDPI AG, pp. 1–18, Nov. 01, 2020. doi: 10.3390/pr8111461.

[13] Y. Marcus, “Some advances in supercritical fluid extraction for fuels, bio-materials and purification,” *Processes*, vol. 7, no. 3. MDPI AG, Mar. 01, 2019. doi: 10.3390/pr7030156.

[14] A. K. Sleiti and W. A. Al-Ammari, “Energy and exergy analyses of novel supercritical CO2 Brayton cycles driven by direct oxy-fuel combustor,” *Fuel*, vol. 294, Jun. 2021, doi: 10.1016/j.fuel.2021.120557.

[15] M. E. Siddiqui, A. A. Taimoor, and K. H. Almitani, “Energy and exergy analysis of the S-CO2 Brayton cycle coupled with bottoming cycles,” *Processes*, vol. 6, no. 9, 2018, doi: 10.3390/pr6090153.

[16] J. Xu *et al.*, “Perspective of S−CO2 power cycles,” *Energy*, vol. 186, Nov. 2019, doi: 10.1016/j.energy.2019.07.161.

[17] Y. Liu, Y. Wang, and D. Huang, “Supercritical CO2 Brayton cycle: A state-of-the-art review,” *Energy*, vol. 189. Elsevier Ltd, Dec. 15, 2019. doi: 10.1016/j.energy.2019.115900.

[18] A. Rogalev, N. Rogalev, V. Kindra, I. Komarov, and O. Zlyvko, “Research and Development of the Combined Cycle Power Plants Working on Supercritical Carbon Dioxide,” *Inventions*, vol. 7, no. 3, Sep. 2022, doi: 10.3390/inventions7030076.

[19] Z. Liu, P. Wang, X. Sun, and B. Zhao, “Analysis on thermodynamic and economic performances of supercritical carbon dioxide Brayton cycle with the dynamic component models and constraint conditions,” *Energy*, vol. 240, Feb. 2022, doi: 10.1016/j.energy.2021.122792.

[20] US Energy Information Adminsitration (EIA), “Country analysis executive summary: iraq,” *US Energy Inf. Adminsitration*, no. January, pp. 1–8, 2022.

[21] E. G. Feher, “The supercritical thermodynamic power cycle,” *Energy Convers.*, vol. 8, no. 2, pp. 85–90, 1968, doi: 10.1016/0013-7480(68)90105-8.

[22] V. Dostal, P. Hejzlar, and M. J. Driscoll, “High-performance supercritical carbon dioxide cycle for next-generation nuclear reactors,” *Nucl. Technol.*, vol. 154, no. 3, pp. 265–282, 2006, doi: 10.13182/NT154-265.

[23] S. Ishiyama, Y. Muto, Y. Kato, S. Nishio, T. Hayashi, and Y. Nomoto, “Study of steam, helium and supercritical CO2 turbine power generations in prototype fusion power reactor,” *Prog. Nucl. Energy*, vol. 50, no. 2–6, pp. 325–332, Mar.

2008, doi: 10.1016/j.pnucene.2007.11.078.

[24] E. M. Clementoni, T. L. Cox, and C. P. Sprague, “Startup and operation of a supercritical carbon dioxide brayton cycle,” *J. Eng. Gas Turbines Power*, vol. 136, no. 7, 2014, doi: 10.1115/1.4026539.

[25] C. S. Turchi, Z. Ma, T. W. Neises, and M. J. Wagner, “Thermodynamic study of advanced supercritical carbon dioxide power cycles for concentrating solar power systems,” *J. Sol. Energy Eng. Trans. ASME*, vol. 135, no. 4, pp. 1–7, 2013, doi: 10.1115/1.4024030.

[26] J. Pasch, T. Conboy, D. Fleming, and G. Rochau, “Brayton Cycle : Completed Assembly Description,” *Sandia Natl. Lab.*, no. October, pp. 1–40, 2012, [Online]. Available: http://www.ntis.gov/help/ordermethods.asp?loc=7-4-0#online

[27] R. J. Allam, J. E. Fetvedt, B. a Forrest, and D. a Freed, “Developments To Produce Even Lower-Cost Electricity From,” *Proc. ASME Turbo Expo 2014 Turbine Tech. Conf. Expo.*, pp. 1–9, 2014.

[28] Y. Le Moullec, “Conceptual study of a high efficiency coal-fired power plant with CO2 capture using a supercritical CO2 Brayton cycle,” *Energy*, vol. 49, no. 1, pp. 32–46, 2013, doi: 10.1016/j.energy.2012.10.022.

[29] G. Lee and B. Lee, “Development of the Supercritical Carbon Dioxide Power Cycle in KIER,” *Proc. ASME Turbo Expo 2017 Turbomach. Tech. Conf. Expo.*, pp. 1–8, 2017.

[30] R. V. Padilla, Y. C. Soo Too, R. Benito, and W. Stein, “Exergetic analysis of supercritical CO2 Brayton cycles integrated with solar central receivers,” *Appl. Energy*, vol. 148, pp. 348–365, Jun. 2015, doi: 10.1016/j.apenergy.2015.03.090.

[31] H. Zhang, H. Zhao, Q. Deng, and Z. Feng, “AEROTHERMODYNAMIC DESIGN AND NUMERICAL INVESTIGATION OF SUPERCRITICAL CARBON DIOXIDE TURBINE,” 2015. [Online]. Available: http://www.asme.org/about-asme/terms-of-use

[32] N. Weiland, W. Shelton, C. White, and D. Gray, “Performance Baseline for Direct-Fired sCO2 Cycles,” *5th Int. Supercrit. CO2 Power Cycles Symp.*, pp. 1–18, 2016.

[33] Q. Zhu, *Power generation from coal using supercritical CO2 cycle.*

[34] J. Cho *et al.*, “Development of the supercritical carbon dioxide power cycle experimental loop with a turbo-generator,” *Proc. ASME Turbo Expo*, vol. 9, pp. 1–8, 2017, doi: 10.1115/GT2017-64287.

[35] J. Cho *et al.*, “Development and Power Generating Operation of the Supercritical Carbon Dioxide Power Cycle Experimental Test Loop in Kier,” *3rd Eur. Supercrit. CO2 Conf.*, pp. 1–10, 2019, doi: 10.17185/duepublico/48905.

[36] K. Wang, M. J. Li, J. Q. Guo, P. Li, and Z. Bin Liu, “A systematic comparison of different S-CO2 Brayton cycle layouts based on multi-objective optimization for applications in solar power tower plants,” *Appl. Energy*, vol. 212, no. December 2017, pp. 109–121, 2018, doi: 10.1016/j.apenergy.2017.12.031.

[37] A. S. Alsagri, A. Chiasson, and M. Gadalla, “Viability assessment of a concentrated solar power tower with a supercritical CO2 Brayton cycle power plant,” *J. Sol. Energy Eng. Trans. ASME*, vol. 141, no. 5, 2019, doi: 10.1115/1.4043515.

[38] J. A. Bennett, J. Fuhrman, T. Brown, N. Andrews, R. Fittro, and A. F. Clarens, “Feasibility of Using sCO2 Turbines to Balance Load in Power Grids with a High Deployment of Solar Generation,” *Energy*, vol. 181, pp. 548–560, Aug. 2019, doi: 10.1016/j.energy.2019.05.143.

[39] M. Astolfi, D. Alfani, S. Lasala, and E. Macchi, “Comparison between ORC and CO2 power systems for the exploitation of low-medium temperature heat sources,” *Energy*, vol. 161, pp. 1250–1261, 2018, doi: 10.1016/j.energy.2018.07.099.

[40] D. A. Politecnico *et al.*, “Optimization of the Part-Load Operation Strategy of SCO2 Power Plants BIONICO View project organic rankine cycle View project OPTIMIZATION OF THE PART-LOAD OPERATION STRATEGY OF SCO2 POWER PLANTS.” [Online]. Available: https://www.researchgate.net/publication/335757847

[41] A. A. Gkountas, L. Th. Benos, K. S. Nikas, and I. E. Sarris, “Heat transfer improvement by an Al2O3-water nanofluid coolant in printed-circuit heat exchangers of supercritical CO2 Brayton cycle,” *Therm. Sci. Eng. Prog.*, vol. 20, no. August, p. 100694, 2020, doi: 10.1016/j.tsep.2020.100694.

[42] J. Yang, Z. Yang, and Y. Duan, “Part-load performance analysis and comparison of supercritical CO2 Brayton cycles,” *Energy Convers. Manag.*, vol. 214, Jun. 2020, doi: 10.1016/j.enconman.2020.112832.

[43] A. Uusitalo, T. Turunen-Saaresti, and A. Grönman, “Design and loss analysis of radial turbines for supercritical CO2 Brayton cycles,” *Energy*, vol. 230, Sep. 2021, doi: 10.1016/j.energy.2021.120878.

[44] S. Chen, Y. Zheng, M. Wu, J. Hu, and W. Xiang, “Thermodynamic analysis of oxy-fuel combustion integrated with the sCO2 Brayton cycle for combined heat and power production,” *Energy Convers. Manag.*, vol. 232, 2021, doi: 10.1016/j.enconman.2021.113869.

[45] M. Chen, R. Zhao, L. Zhao, D. Zhao, S. Deng, and W. Wang, “Supercritical CO2 Brayton cycle: Intelligent construction method and case study,” *Energy Convers. Manag.*, vol. 246, Oct. 2021, doi: 10.1016/j.enconman.2021.114662.

[46] D. Alfani, M. Binotti, E. Macchi, P. Silva, and M. Astolfi, “sCO2 power plants for waste heat recovery: Design optimization and part-load operation strategies,” *Appl. Therm. Eng.*, vol. 195, Aug. 2021, doi:

10.1016/j.applthermaleng.2021.117013.

[47] T. Gotelip, U. Gampe, and S. Glos, “Optimization strategies of different SCO2 architectures for gas turbine bottoming cycle applications,” *Energy*, vol. 250, p. 123734, Jul. 2022, doi: 10.1016/j.energy.2022.123734.

[48] S. Khatoon and M. H. Kim, “Preliminary design and assessment of concentrated solar power plant using supercritical carbon dioxide Brayton cycles,” *Energy Convers. Manag.*, vol. 252, Jan. 2022, doi: 10.1016/j.enconman.2021.115066.

[49] F. Witte and I. Tuschy, “TESPy: Thermal Engineering Systems in Python,” *J. Open Source Softw.*, vol. 5, no. 49, p. 2178, 2020, doi: 10.21105/joss.02178.

[50] F. Witte, M. Hofmann, J. Meier, I. Tuschy, and G. Tsatsaronis, “Generic and Open-Source Exergy Analysis—Extending the Simulation Framework TESPy,” *Energies*, vol. 15, no. 11, Jun. 2022, doi: 10.3390/en15114087.

[51] Sven Erik Jørgensen, *No Title*. 2004.

[52] K. Seshadri, “Thermal design and optimization,” *Energy*, vol. 21, no. 5, pp. 433–434, 1996, doi: 10.1016/s0360-5442(96)90000-6.

[53] T. Morosuk and G. Tsatsaronis, “Splitting physical exergy: Theory and application,” *Energy*, vol. 167, pp. 698–707, 2019, doi: 10.1016/j.energy.2018.10.090.

[54] M. Penkuhn and G. Tsatsaronis, “The 5 th International Symposium-Supercritical CO 2 Power Cycles Exergy Analysis of the Allam Cycle,” pp. 1–18, 2016.

[55] C. K. Ho, M. Carlson, P. Garg, and P. Kumar, “Cost and performance tradeoffs of alternative solar-driven s-CO2 Brayton cycle configurations,” *ASME 2015 9th Int. Conf. Energy Sustain. ES 2015, collocated with ASME 2015 Power Conf. ASME 2015 13th Int. Conf. Fuel Cell Sci. Eng. Technol. ASME 2015 Nucl. Forum*, vol. 1, pp. 1–10, 2015, doi: 10.1115/ES2015-49467.

[56] H. H. Zhu, K. Wang, and Y. L. He, “Thermodynamic analysis and comparison for different direct-heated supercritical CO2 Brayton cycles integrated into a solar thermal power tower system,” *Energy*, vol. 140, pp. 144–157, 2017, doi: 10.1016/j.energy.2017.08.067.

[57] IPCC, *Revised 1996 IPCC Guidelines for National Greenhouse Gas Inventories*. 1996. [Online]. Available: https://www.ipcc-nggip.iges.or.jp/public/gl/pdfiles/invs2a.pdf

[58] “QTR2015-4R-Supercritical-Carbon-Dioxide-Brayton Cycle (1)”.

[59] J. J. Moore, S. Cich, M. Towler, T. Allison, J. Wade, and D. Hofer, “Commissioning of a 1 MWe Supercritical CO 2 Test Loop,” *6th Int. Symp. - Supercrit. CO2 Power Cycles*, pp. 1–36, 2018.

[60] S. Wright, R. Radel, M. Vernon, P. Pickard, and G. Rochau, “Operation and analysis of a supercritical CO2 Brayton cycle.,” Albuquerque, NM, and Livermore, CA (United States), Sep. 2010. doi: 10.2172/984129.

[61] Y. Ahn *et al.*, “Review of supercritical CO2 power cycle technology and current status of research and development,” *Nucl. Eng. Technol.*, vol. 47, no. 6, pp. 647–661, 2015, doi: 10.1016/j.net.2015.06.009.

[62] J. Cho *et al.*, “Preliminary power generating operation of the supercritical carbon dioxide power cycle experimental test loop with a turbo-generator,” *6th Int. Symp. CO2 Power Cycles*, pp. 27–29, 2018.

RESUME

This is Zainalabden Oday Hatm MOHMEDALIALNAJFY, a mechanical engineer, graduated in 2019 from the Al-furat alawest Technical University Collage of Engineering, the Department of Power Mechanic Technology, and was ranked first in his department and the Engineering College as a whole, and was assigned to work at the same university, in 2021 he started his master's study at the Karabuk University, Department of Mechanical Engineering.